

PLOS Pathogens

Whole genome sequencing of *Borrelia burgdorferi* isolates reveals linked clusters of plasmid-borne accessory genome elements associated with virulence.

--Manuscript Draft--

Manuscript Number:	PPATHOGENS-D-23-00364
Full Title:	Whole genome sequencing of <i>Borrelia burgdorferi</i> isolates reveals linked clusters of plasmid-borne accessory genome elements associated with virulence.
Short Title:	<i>Borrelia burgdorferi</i> genomes reveal linked clusters of accessory elements linked to virulence
Article Type:	Research Article
Section/Category:	Gram Negative Bacteria
Keywords:	Lyme disease, <i>Borrelia burgdorferi</i> , Whole Genome Sequencing; Virulence; Pathogenicity
Abstract:	<p>Lyme disease is the most common vector-borne disease in North America and Europe. The clinical manifestations of Lyme disease vary based on the genospecies of the infecting <i>Borrelia burgdorferi</i> spirochete, but the microbial genetic elements underlying these associations are not known. Here, we report the whole genome sequence (WGS) and analysis of 299 patient-derived <i>B. burgdorferi sensu stricto</i> (Bbss) isolates from patients in the Eastern and Midwestern US and Central Europe. We develop a WGS-based classification of Bbss isolates, confirm and extend the findings of previous single- and multi-locus typing systems, define the plasmid profiles of human-infectious Bbss isolates, annotate the core and strain-variable surface lipoproteome, and identify loci associated with disseminated infection. A core genome consisting of ~800 open reading frames and a core set of plasmids consisting of lp17, lp25, lp36, lp28-3, lp28-4, lp54, and cp26 are found in nearly all isolates. Strain-variable (accessory) plasmids and genes correlate strongly with phylogeny. Using genetic association study methods, we identify an accessory genome signature associated with dissemination and define the individual plasmids and genes that make up this signature. Strains within the RST1/WGS A subgroup, particularly a subset marked by the OspC type A genotype, are associated with increased rates of dissemination. OspC type A strains possess a unique constellation of strongly linked genetic changes including the presence of lp56 and lp28-1 plasmids and a cluster of genes that may contribute to their enhanced virulence compared to other genotypes. The patterns of OspC type A strains typify a broader paradigm across Bbss isolates, in which genetic structure is defined by correlated groups of strain-variable genes located predominantly on plasmids, particularly for expression of surface-exposed lipoproteins. These clusters of genes are inherited in blocks through strain-specific patterns of plasmid occupancy and are associated with the probability of invasive infection.</p>
Additional Information:	
Question	Response
<p>Government Employee</p> <p>Are you or any of the contributing authors an employee of the United States government?</p> <p>Manuscripts authored by one or more US Government employees are not copyrighted, but are licensed under a CC0 Public Domain Dedication, which allows unlimited distribution and reuse of the</p>	<p>No - No authors are employees of the U.S. government.</p>

<p>article for any lawful purpose. This is a legal requirement for US Government employees.</p> <p>This will be typeset if the manuscript is accepted for publication.</p>	
<p>Financial Disclosure</p> <p>Enter a financial disclosure statement that describes the sources of funding for the work included in this submission and the role the funder(s) played. This includes grants and any commercial funding of the work or authors.</p> <p>This statement will be typeset if the manuscript is accepted for publication.</p> <p>Review the submission guidelines and the instructions link below for detailed requirements and guidance.</p>	<p>This work was supported by a Doris Duke Charitable Foundation Physician Scientist Fellowship (to J.E.L), the National Institute of Allergy and Infectious Diseases (K99/R00148604 to J.E.L, U19AI110818 and U01 AI151812 to P.C.S.; R01AI045801 to I.S., and R21AI144916 to K.S.), the National Institute of Arthritis and Musculoskeletal and Skin Diseases (R01AR41511 to I.S. and K01AR062098 to K.S.), the Bay Area Lyme Foundation (to P.C.S. and J.E.L.), the Howard Hughes Medical Institute (P.C.S.), the Arthritis Foundation Fellowship (to K.S.), and the Slovenian Research Agency (P3-0296, J3-1744, and J3-8195 to F.S.).</p>
<p>Competing Interests</p> <p>On behalf of all authors, disclose any competing interests that could be perceived to bias this work.</p> <p>This statement will be typeset if the manuscript is accepted for publication.</p> <p>Review the instructions link below and PLOS Pathogens' competing interests policy to determine what information must be disclosed at submission.</p>	<p>P.C.S. is a co-founder of, shareholder in, and consultant to Sherlock Biosciences and Delve Bio, as well as a board member of and shareholder in Danaher Corporation. K.S. served as a consultant for T2 Biosystems, Roche, BioMerieux, and NYS Biodefense Fund, for the development of a diagnostic assay in Lyme borreliosis. F.S. served on the scientific advisory board for Roche on Lyme disease serological diagnostics and on the scientific advisory board for Pfizer on Lyme disease vaccine, and is an unpaid member of the steering committee of the ESCMID Study Group on Lyme Borreliosis/ESGBOR. J.A.B. has received research funding from Analog Devices Inc., Zeus Scientific, Immunetics, Pfizer, DiaSorin and bioMerieux, and has been a paid consultant to T2 Biosystems, DiaSorin, and Roche Diagnostics. G.P.W. reports receiving research grants from Institute for Systems Biology, Biopeptides, Corp., and Pfizer, Inc. He has been an expert witness in malpractice cases involving Lyme disease and babesiosis; and is an unpaid board member of the non-profit American Lyme Disease Foundation.</p>
<p>Data Availability</p> <p>Provide a Data Availability Statement in the box below. This statement should detail where the data used in this submission can be accessed. This statement will be typeset if the manuscript is accepted for publication.</p>	<p>Genome sequences reported here have been deposited in Genbank under PRJNA923804. Code is available at https://github.com/JacobLemieux/borreliaseq.</p>

Before publication, authors are required to make all data underlying their findings fully available, without restriction. Review our [PLOS Data Policy](#) page for detailed information on this policy. Instructions for writing your Data Availability statement can be accessed via the Instructions link below.

1 **Title:** Whole genome sequencing of *Borrelia burgdorferi* isolates reveals linked clusters of
2 plasmid-borne accessory genome elements associated with virulence.

3

4 Jacob E. Lemieux^{1,2}, Weihua Huang^{3,4}, Nathan Hill^{1,2}, Tjasa Cerar⁵, Lisa Freemark², Sergio
5 Hernandez⁶, Matteo Luban^{1,2}, Vera Maraspin⁷, Petra Bogovic⁷, Katarina Ogrinc⁷, Eva Ruzic-
6 Sabljic⁵, Pascal Lapierre⁶, Erica Lasek-Nesselquist⁶, Navjot Singh⁶, Radha Iyer³, Dionysios
7 Liveris³, Kurt D. Reed⁸, John M. Leong⁹, John A. Branda¹, Allen C. Steere¹, Gary P. Wormser³,
8 Franc Strle⁷, Pardis C. Sabeti^{1,2,10,11*}, Ira Schwartz^{3,*}, and Klemen Strle^{1,6,*}

9

10 ¹Massachusetts General Hospital, Harvard Medical School, ²Broad Institute of MIT and Harvard,
11 ³New York Medical College, ⁴East Carolina University, ⁵University of Ljubljana, ⁶Wadsworth
12 Center, ⁷University Medical Center Ljubljana, ⁸University of Wisconsin, ⁹Tufts University,
13 Department of Molecular Biology and Microbiology ¹⁰Harvard University, ¹¹Harvard T.H.Chan
14 School of Public Health.

15 *Contributed equally to this work

16 Correspondence to: lemieux@broadinstitute.org

17 Key words: Lyme disease, *Borrelia burgdorferi*, Whole Genome Sequencing; Virulence;
18 Pathogenicity

19

20

21

22 **Abstract:** Lyme disease is the most common vector-borne disease in North America and
23 Europe. The clinical manifestations of Lyme disease vary based on the genospecies of the
24 infecting *Borrelia burgdorferi* spirochete, but the microbial genetic elements underlying these
25 associations are not known. Here, we report the whole genome sequence (WGS) and analysis
26 of 299 patient-derived *B. burgdorferi* sensu stricto (*Bbss*) isolates from patients in the Eastern
27 and Midwestern US and Central Europe. We develop a WGS-based classification of *Bbss*
28 isolates, confirm and extend the findings of previous single- and multi-locus typing systems,
29 define the plasmid profiles of human-infectious *Bbss* isolates, annotate the core and strain-
30 variable surface lipoproteome, and identify loci associated with disseminated infection. A core
31 genome consisting of ~800 open reading frames and a core set of plasmids consisting of lp17,
32 lp25, lp36, lp28-3, lp28-4, lp54, and cp26 are found in nearly all isolates. Strain-variable
33 (accessory) plasmids and genes correlate strongly with phylogeny. Using genetic association
34 study methods, we identify an accessory genome signature associated with dissemination and
35 define the individual plasmids and genes that make up this signature. Strains within the
36 RST1/WGS A subgroup, particularly a subset marked by the OspC type A genotype, are
37 associated with increased rates of dissemination. OspC type A strains possess a unique
38 constellation of strongly linked genetic changes including the presence of lp56 and lp28-1
39 plasmids and a cluster of genes that may contribute to their enhanced virulence compared to
40 other genotypes. The patterns of OspC type A strains typify a broader paradigm across *Bbss*
41 isolates, in which genetic structure is defined by correlated groups of strain-variable genes
42 located predominantly on plasmids, particularly for expression of surface-exposed lipoproteins.
43 These clusters of genes are inherited in blocks through strain-specific patterns of plasmid
44 occupancy and are associated with the probability of invasive infection.

45 INTRODUCTION

46 Lyme disease is a heterogeneous illness caused by spirochetes of the *Borrelia burgdorferi*
47 sensu lato (~~*Bbsl*, sensu lato meaning 'in the broad sense'~~) complex. *Bbsl* contains over 20
48 ~~subspecies (also termed genospecies, genomic species)~~, four of which cause the majority of
49 disease in humans: *B. burgdorferi* sensu stricto (~~*Bbss*, sensu stricto meaning in the strict~~
50 ~~sense~~), *B. afzelii*, *B. garinii*, and *B. bavariensis* [1]. **Nearly all** Lyme disease in the US is caused
51 by *Bbss*. In Europe, **most** infections are caused by *B. afzelii*, *B. garinii*, or *B. bavariensis*,
52 whereas infection due to *Bbss* is **rare**. Infection with *Bbsl* **usually** presents as an expanding skin
53 rash, erythema migrans (EM), at the site of the tick-bite. If untreated, spirochetes may
54 disseminate to secondary sites (~~a phenotype described as 'dissemination'~~), primarily other skin
55 sites, the nervous system and joints [1,2]. In addition to clinical variation among *Bbsl* species,
56 differences in virulence have also been noted between genotypes within *Bbss* [3–5], and such
57 phenotypes have been recapitulated in murine models [6–8]. These associations imply that
58 microbial genetic loci likely influence the clinical manifestations of Lyme disease. Despite such
59 evidence linking microbial genotype to clinical phenotype, the specific genes or loci responsible
60 for the clinical manifestations of Lyme disease have not yet been identified.

61 *Bbss* genome analysis has been limited to date due to technical challenges of
62 sequencing and assembly and difficulties of obtaining isolates from cases of human disease.
63 The *Bbss* genome consists of a roughly one megabase of core genome (consisting of a ~900Kb
64 chromosome and the plasmids cp26 and lp54), as well as numerous (>15) additional circular
65 and linear ~~extrachromosomal DNA elements (colloquially termed plasmids)~~ [9,10]. Subsets of
66 plasmids have high levels of homology (as exemplified by seven 32 kilobase circular plasmids
67 (cp32) [11] and four 28-kilobase linear plasmids (lp28) [10] in the B31 reference isolate), which
68 have diversified through duplication, recombination, and other ~~primordial~~ evolutionary events
69 [12]. The sheer number of plasmids and their extreme homology has made sequencing and

70 assembly of complete *Bbss* genomes a major challenge, particularly with widely-used short read
71 sequencing methods [13].

72 The technical challenges of sequencing and assembly are compounded by the difficulty
73 of obtaining isolates from human disease. It ~~has been~~^{is} possible to culture the organism from EM
74 lesions in the majority of cases, but this requires a skin biopsy and specialized culture
75 techniques, both of which are rarely used in routine clinical practice. The organism has
76 occasionally been cultured from CSF in patients with meningitis, but ~~extremely~~ rarely from
77 synovial fluid in patients with Lyme arthritis, the most common late disease manifestation in the
78 US. Thus, the ~~great~~ majority of available *Bbss* isolates are from patients with EM, an early
79 disease manifestation. As a result of these challenges, only a small number of human clinical
80 isolates have been sequenced and analyzed. To our knowledge, no large WGS studies of
81 human isolates have been conducted. Fewer than 50 human isolates analyzed by WGS have
82 been publicly reported, either sporadically or included in cohorts consisting primarily of tick-
83 derived isolates [14–19].

84 Genotyping systems have been developed to subclassify *Bbss* strains using single or
85 multiple genomic regions (reviewed in [20]). Two of the most commonly used typing methods
86 are based on a restriction-fragment length polymorphisms in the 16S-23S ribosomal RNA
87 spacer region [21,22], termed ribosomal spacer type (RST), and on sequence variation of outer
88 surface protein C (OspC), one of the most variable *Bbss* proteins [23,24]. RST typing subdivides
89 *Bbss* into 3 types, referred to as RST1, RST2 and RST3 [6], whereas OspC typing subdivides
90 *Bbss* into ~30 OspC genotypes of which >24 cause infection in humans [25–27]. RST and OspC
91 are in linkage disequilibrium on the core genome, and each RST genotype is generally
92 associated with particular OspC types (e.g., RST1 mostly corresponds to OspC types A and B
93 and RST2 corresponds primarily to OspC types F, H, K and N) [27]), whereas RST3 is the most
94 variable and correlates with the remaining OspC types. In addition to these genotyping

95 methods, multilocus sequence typing (MLST), which is based on eight chromosomal
96 housekeeping genes, has been used to further sub-stratify the strains [27,28]. According to the
97 *Borrelia* MLST database (<https://pubmlst.org/borrelia/>), >900 MLST sequence types have been
98 identified.

99 Application of targeted genotyping methods has previously established a link between
100 *Bbss* microbial genotype and several phenotypic properties including dissemination, disease
101 severity, immunogenicity, and distinct clinical presentation [1,3,5,6,8,26,27,29–32]. For
102 example, using RST and OspC genotyping we previously showed that RST1 OspC type A
103 strains have greater proclivity to disseminate, are more immunogenic, are associated with more
104 symptomatic early infection, and with a greater frequency of post-infectious Lyme arthritis.
105 However, these approaches lack the resolution to reconstruct a detailed evolutionary history or
106 to define individual genes or loci underlying phenotypic variability. The limitations of previous
107 studies have been further compounded by the absence of large cohorts of patient-derived
108 isolates accompanied by detailed clinical information. Here, we used whole genome sequencing
109 to characterize in detail the genomes – including the core genome and associated plasmids – of
110 299 patient-derived *Bbss* strains. The isolates were collected primarily from patients with EM,
111 ~~the initial skin lesion of the infection,~~ over three decades across Northeastern and Midwestern
112 US and Central Europe. We carried out phylogenetic and phylogeographic analysis, and
113 identified particular *Bbss* genomic groups, plasmids, and individual open reading frames (ORFs)
114 associated with ~~tissue invasive (disseminated)~~ human disease.

115

116 **MATERIALS and METHODS**

117 **Selection of *B. burgdorferi* isolates (see Supplemental Table 1).** In total, 299 *Bbss* isolates
118 collected from 299 patients over a 30-year period (1992-2021) were included in this study: 202

119 from the Northeastern US, 61 from the Midwestern US and 36 from Slovenia (Central Europe).
120 The majority (97%) of isolates were derived from skin (n = 287) or blood (n = 2) of patients (9
121 were derived from ~~cerebrospinal fluid~~ [CSF]) by culturing in BSK or MKP medium [33,34]. All
122 patients met the US Centers for Disease Control and Prevention (CDC) criteria for Lyme
123 disease [35]. Only low passage isolates (passage <5) were used for WGS.

124 *Northeastern United States:* The 201 isolates from the Northeastern US were collected at two
125 geographic locations: 113 from New England (primarily from contiguous regions of
126 Massachusetts, Rhode Island, and Connecticut) and 88 from New York State. The New York
127 strains belong to a larger collection of more than 400 clinical isolates, collected between 1992-
128 2005, that had been previously typed at the *rrs-rrlA* IGS and *ospC* loci [4,31]. To account for the
129 full diversity of *Bbss* genotypes found in the collection, isolates with the best sequence quality
130 from each *OspC* major group were selected for this study in accordance with their prevalence in
131 the entire collection. All of the latter isolates were cultured from skin biopsies of infected
132 patients, rather than from blood or CSF (Supplemental Tables 1 and 2).

133 *Midwestern United States:* The 62 isolates from the Midwestern US were derived from
134 specimens submitted to the Marshfield Laboratories (Marshfield, WI) for *Borrelia* culture from
135 1993 to 2003 (Supplemental Tables 1 and 2).

136 *Central Europe (Slovenia):* The 36 isolates from Slovenia represent all *Bbss* isolates that were
137 cultured from patients over a 27-year period (1994-2021), who were evaluated at the Lyme
138 borreliosis outpatient clinic at the University Medical Center Ljubljana (UMCL).

139

140 **Selection of patients.** This study involves secondary use of deidentified archival clinical
141 isolates and patient data collected in previous studies and was approved by the Massachusetts

142 General Hospital Institutional Review Board (IRB) under protocol 2019P001864. Patients
143 included in this study were diagnosed with early Lyme disease and were classified as having
144 either localized or disseminated infection. Early Lyme disease was defined by the presence of at
145 least one EM skin lesion or symptoms consistent with Lyme neuroborreliosis along with a
146 positive CSF culture. Localized infection was defined by a single culture positive EM skin lesion
147 in the absence of clinical and/or microbiological evidence of dissemination to a secondary site.
148 Disseminated infection was defined by a positive blood or CSF culture or PCR, multiple EM
149 lesions, and/or signs of neurological involvement. We were able to classify 291 or the 299
150 (97.3%) isolates as Disseminated or Localized by these criteria. Clinical records were not
151 available to classify 8/299 (2.7%), and these isolates were excluded from analyses of
152 dissemination. A measure of bloodstream dissemination was available for 212/299 (70.9%) of
153 isolates, with blood PCR available for 106/299 (35.4%) and blood culture available for a disjoint
154 set of 106/299 (35.4%) of all isolates. Multiple EM was present in 57 / 290 (19.7%); among
155 patients with a single EM, 23/88 (26.1%) had a positive blood culture and 28/86 (32.6%) had a
156 positive PCR. Complications such as Lyme neuroborreliosis were defined by clinical criteria and
157 based on assessment by the treating clinician. In Europe, central nervous system (CNS)
158 pleocytosis and intrathecal production of *Borrelia* antibodies were required for diagnostic
159 determination of Lyme neuroborreliosis, following the EFNS guidelines [36]. Summary statistics
160 of isolates by group is provided in Supplemental Table 1. The list of isolates and associated
161 metadata is provided in Supplemental Table 2.

162 **Whole-Genome Sequencing.** *Bbss* DNA was isolated from the cultured isolates with either the
163 IsoQuick kit (Orca Research, Bothell, WA), the Gentra PureGene DNA Isolation Kit (Qiagen
164 Inc., Valencia, CA), or the DNEasy kit (Qiagen Inc, Valencia, CA). Short-read next-generation

165 sequencing (NGS) library construction was performed using the Nextera XT Library Prep Kit
166 (Illumina, San Diego, CA). DNA quantification was performed ~~in a 96-well microplate~~ using the
167 SpectraMax Quant dsDNA Assay Kit and the Gemini XPS Fluorometer (Molecular Devices, San
168 Jose, CA), or ~~in a single tube~~ using the Qubit 2.0 fluorometer (Thermo Fisher Scientific,
169 Springfield Township, NJ). Library quality was examined using the 4200 TapeStation and D1000
170 ScreenTape (Agilent, Santa Clara, CA). Paired-end sequencing (2 × 150 or 250 cycles) was
171 performed using the NextSeq 550 or MiSeq system (Illumina).

172 **Bioinformatics Data Analysis.** Trimmomatic v0.39 [37] was used for trimming and cleaning of
173 raw sequence reads; SPAdes v3.14.1 [38] for *de novo* genome assembly; QUAST [39] for
174 quality assessment and assembly visualization; Kraken2 [40] v2.1.1 for digital cleaning of
175 assembled genomic sequence by using taxonomy classification; mlst v2.19.0
176 (<https://github.com/tseemann>) for MLST [41] identification from assembled sequences; k-mer
177 weighted inner product (kWIP) [42] v0.2.0 for alignment-free, k-mer-based relatedness analysis;
178 prokka v1.14.6 [43] for genome sequence annotation; Roary [44] for core- and pan-genome
179 analysis; FastTree v2.1.11 [45] for phylogeny tree generation. Bioconductor [46] packages in R
180 [47] v4.1.1 and/or RStudio v2021.09.0+351, such as ggplot2 [48], ggtree [49], ggtreeExtra, and
181 ggstar, were also used for phylogeny tree generation. MLST definitions were downloaded from
182 pubMLST. Multidimensional scaling (MDS) was calculated on the kWIP distances using the
183 command `mdscale()` in R. Fisher's exact test was used for pairwise comparison of categorical
184 variables using the `fisher.test()` function in R. The MiniKraken2 database was constructed for
185 Kraken2 from complete bacterial, archaeal, and viral genomes in RefSeq as of March 12, 2020.
186 To characterize the plasmid content of individual isolates, we took two approaches. We first
187 aligned the contigs to the B31 reference and quantified a plasmid as present or absent if greater

188 than 50% of the reference genome plasmid was covered by contigs. As a complementary
189 approach, we built a hidden Markov model (HMM) of PFam32 genes using HMMer [50] and
190 searched the resulting profile against the assemblies to identify PFam32 genes. We then
191 aligned the resulting putative PFam32 genes against a set of canonical PFam32 genes,
192 provided by Dr. Sherwood Casjens, that have been used to determine plasmid types in
193 published reports [51]. For each putative PFam32 gene, if a match with <5% identity was
194 present in the list of annotated PFam32 genes, we marked the isolate as having a copy of the
195 closest-matching PFam32 based on sequence identity. If no PFam32 within these thresholds
196 could be identified, the closest PFam32 family member was considered unknown and not
197 assigned in this analysis.

198

199 RESULTS

200 *Whole-genome sequencing of human Borrelia burgdorferi sensu stricto isolates*

201 To gain insight into the evolution, population structure, and pathogenesis of *Bbss* in human
202 infection, we sequenced the complete genomes of 299 *Bbss* from human cases of early Lyme
203 disease. We sequenced their whole genomes at a median coverage of 57.6x (interquartile
204 range [IQR] 27.6x - 130.8x). The *de novo* assemblies produced high-quality, nearly-complete
205 genomic assemblies with a median total length of 1.34 megabases (Mb) (IQR 1.30 - 1.37 Mb).
206 Final assemblies contained a median of 107 contigs per isolate (IQR 88.0 - 137.5) and had a
207 median N50 of 213,476 bases (IQR 80,809 - 221,506 bases). We were unable to finish
208 assembly of plasmids due to repetitive plasmid sequences. Assembly statistics are given in
209 Supplemental Table 3.

210 As an initial characterization of divergence between strains without any reference or
211 annotation, we applied alignment-free, kmer-based analysis (kWIP) to the WGS data and

212 identified three major clusters based on their genetic distances (Figure 1C and D, Figure S1).
213 This unbiased distance analysis revealed that a single lineage (WGS A) was divergent from all
214 other isolates (Figure 1C and D). The remaining isolates are grouped into two stable clusters
215 (WGS groups B and C). RST type 1 was divergent from the other two WGS groups, but RST 2
216 and 3 were mixed between WGS groups B and C (Figures 1C and 1D).

217 We next constructed both maximum-likelihood (ML) and maximum clade credibility
218 (MCC) phylogenetic trees using core genome elements (as defined by Roary[44], see methods)
219 from WGS (Figure 2). WGS groups defined by k-mer distance corresponded to the ML clade
220 structure on the core-genome tree and the associated OspC types (Figure 2A and E). However,
221 they revealed substructure within these groups, particularly WGS group B, which we split into
222 subclusters B.1 and B.2 (Figure 2B and S3B). We also inferred MCC trees using Bayesian
223 methods as implemented in BEAST. A MCC tree is shown in Figure S2; ML and MCC trees
224 were in broad agreement, and the posterior probability of all nodes separating WGS groups was
225 > 0.99, indicating that the distance-based clustering was phylogenetically well-supported.

226

227 *Comparison of Bbss isolates using classical genotyping approaches*

228 We typed these isolates using the RST, OspC, and MLST typing schemes and compared WGS
229 type to these existing methods (Figures 1A and 1B). Among the 299 strains, 98 were RST1
230 (32.7%), 112 were RST2 (37.4%), and 89 (29.8%) were RST3; 52 (17%) were OspC type K, 44
231 (15%) were OspC type A, 46 (15%) were OspC type B, and 21 (7%) were OspC type H. As
232 demonstrated previously [4,30], there was a strong linkage between RST and OspC type
233 (Fisher's exact test, $p < 1 \times 10^{-6}$).

234 In Slovenia in Europe, the most common isolates were RST1 (75%), >60% of which
235 were OspC type B. In contrast, the most common *Bbss* isolates in the US were RST2 (41% in

236 Northeastern US and 49% in Midwestern US), whereas RST1 strains comprised 32% of the
237 strains in Northeastern US and only 10% in the Midwest. Further, certain OspC types have
238 distinct geographic distributions. For example, OspC type L is found only in the Midwestern US
239 and Slovenia and OspC types Q, R and S have only been isolated from European patients
240 [26,27]. These findings are consistent with previous reports that found genetic differences in
241 *Bbss* populations based on geography [26,27]. WGS groups were strongly associated with RST
242 (Figures 1A-B, Fisher's exact test, $p < 1 \times 10^{-6}$) and OspC type (Figure 1A-B, S1; Fisher's exact
243 test, $p < 1 \times 10^{-6}$). RST1 / Osp C type A/B sequences consistently clustered as a single clade in
244 the core genome phylogenetic tree and MDS of k-mer distances (Figures 1C and S1),
245 demonstrating agreement between typing methods. In contrast, RST2 and RST3 were both
246 polyphyletic in the WGS data and contained within separate WGS groups (Figures 1C and 1D).
247 Trees inferred from core genome sequences (Figure 2D, left panel) differed in the relatedness
248 of major clades from those inferred from accessory genome sequences (as defined by Roary
249 [44], see methods) (Figure 2D, right panel), but agreed on the substructure and sample
250 membership of individual clades. This pattern, which affects major clades as a whole, indicates
251 the occurrence of recombination events deep in the evolutionary history between core and
252 accessory genome sequences.

253 Similarly, OspC types were monophyletic on the WGS tree (Figure 2E) and on a tree
254 built from OspC sequences (Figure 2F), but WGS type was polyphyletic on the OspC tree
255 (Figure 2G). Consistent with this polyphyly, face-to-face comparison of core genome and OspC
256 trees demonstrated that in many cases, closely related OspC sequences were part of distinct
257 WGS groups (Figure 2H). For example, the OspC type L isolates from the Midwestern US and
258 Slovenia are on different branches of the core genome phylogenetic tree (Figure S2H). Thus,
259 RST and OspC typing methods identify substructure in *Bbss* genomes, and largely agree on the

260 divergent RST1 / OspC A/B clade. In contrast, RST does not capture fine-grain genetic
261 structure, and OspC sequence distance does not correlate with genome-wide distance between
262 isolates.

263

264 *Population geographic structure:*

265 We next explored the relationship between genetic markers and geography. WGS group was
266 strongly associated with broad geographic region (US Northeast, US Midwest, EU Slovenia)
267 (Fisher's exact test, $p < 1 \times 10^{-6}$), similar to the findings with previously evaluated genetic
268 markers including RST (Fisher's exact test, $p < 1 \times 10^{-6}$) and OspC type (Fisher's exact test, $p <$
269 1×10^{-6}) (counts by geographic region are shown in Figures 1A-B).

270 Using finer-grained geographic clustering among subregions in the Northeastern US
271 (New York, Massachusetts, Connecticut, and Rhode Island), geographic region was significantly
272 associated with WGS group (Fisher's exact test, $p = 0.009$), suggesting that geographic
273 structuring of genotypes also occur on a regional scale (Figure S2E). The number of ORFs in
274 the genome differed significantly by region within a given WGS group (Figure 3A). In the US
275 Northeast and in Slovenia, WGS groups differed significantly by the number of ORFs (Figure
276 3B). As core genome size is relatively constant among strains regardless of geographic
277 location, the differences in accessory genome size across different populations, even within a
278 given genomic group with a single common ancestor, suggests that the diversification of
279 accessory genome size may be one mechanism by which strains adapt to distinct ecological
280 factors in each geographic region. Slovenian isolates are clustered in two well-defined
281 monophyletic groups (Figure 2C), suggesting at least two inter-continental exchanges (Figure
282 S2C), consistent with a previous report [15]. There were numerous (>10) exchanges between
283 samples in the US midwest and northeast (Figure S2D).

284 We attempted to define the timing of these exchanges by inferring a time-stamped
285 phylogeny using BEAST (Supplemental Note 1). Together, these models demonstrate a remote
286 (hundreds of thousands to tens of millions of years) TMRCA for human-infectious strains of
287 *Bbss*, consistent with previous estimates [52]. Precise timing requires more accurate knowledge
288 of the mutation rate in *Bbss*.

289

290 *Associations between genotype and Bbss dissemination in patients:*

291 Dissemination is a crucial clinical event that enables the progression of disease from an EM skin
292 lesion to more severe Lyme disease complications such as meningitis, carditis, and arthritis.

293 Given the previously-reported associations between single-locus genetic markers and
294 dissemination[4,5,8,30], we investigated the relationship between genotype and dissemination.

295 We scored isolates as either disseminated or localized based on certain clinical characteristics
296 of the patients from whom they were obtained, particularly having multiple vs 1 EM skin lesion
297 and having neurologic Lyme disease as well as having positive culture or PCR results for *Bbss*
298 in blood.

299 WGS groups differed from each other in their propensity to disseminate ($p = 0.059$ for 3
300 groups; $p = 0.012$ for 4 groups, Fisher's exact test) (Figure 3C, Figure S3C). Slovenian isolates
301 disseminated at a lower rate (25%) than US isolates (42.7%) ($p = 0.045$, Fisher's exact test),
302 and the relationship between WGS groups and dissemination was slightly stronger when testing
303 US isolates only ($p = 0.02$ for 3 groups; $p = 0.004$ for 4 groups, Fisher's exact test). WGS group
304 A isolates from the US, which correlate with OspC type A and RST1 strains, showed the highest
305 rate of dissemination (51.4%) whereas US WGS group B isolates had the lowest rate of
306 dissemination (32.4%). Within WGS group B, there was evidence of substructure (Figure S3).
307 US B.1 isolates disseminated at a higher rate (40.0%) than B.2 isolates (18.4%) (Figure S3C).


308 Consistent with previous observations [3,4] and with the general alignment of WGS,
309 RST, and OspC type, RST type was also associated with dissemination ($p = 0.010$, Fisher's
310 exact test), with RST1 having the greatest propensity to disseminate and RST3 the lowest [4,5]
311 (Figure S4B). OspC type A was also associated with dissemination ($p = 0.008$, Fisher's exact
312 test, Figure S4A). A significant association with dissemination could not be detected when OspC
313 type was tested as a categorical variable with 23 categories ($p = 0.3$, Fisher's exact test, Figure
314 S4), but power is reduced by many categories.

315 The propensity to disseminate varied greatly among the US and Slovenian isolates,
316 which is likely due to the major genetic differences in isolates between the two regions (Figure
317 3C). In Slovenia, the predominant WGS group A isolates are OspC type B and all the WGS-B.2
318 isolates are **ospC** type L (Figure S4). This correlation was particularly notable for **WGSA** strains,
319 which were recovered from patients with disseminated Lyme disease at a rate of 51.4% in the
320 US vs 23.1% in Slovenia. WGS-B.2 isolates in the US possess the lowest dissemination rate
321 (18.4%), whereas those from Slovenia showed a higher dissemination rate of 30% (Figure 3D
322 and S4A). Taken together, these data confirm that rates of dissemination vary by genotype and
323 demonstrate that WGS A/RST1, particularly a subset distinguished by OspC type A strains, is a
324 genetically distinct lineage with higher rates of dissemination.

325

326 *Plasmid associations with WGS profiles:*

327 As most of the genetic variation in *Bbss* occurs on plasmids [51,53,54], we investigated the
328 variation in plasmid content across genotypes. Assembly and analysis of plasmid sequences is
329 challenging because the length of repeated sequences in plasmids is greater than the read
330 length generated by the short-read Illumina sequencing technology used in this study [13]. To
331 circumvent this, we exploited the relationship between plasmid partition genes (plasmid family



332 32; PFam32) and plasmid types [12,51], putatively identifying the presence or absence of a
333 plasmid by the presence/absence of unique PFam32 sequences (Figure 4). After annotating all
334 PFam32 genes in the assemblies using an HMM, we linked each putative PFam32 to a plasmid
335 by finding the closest match by sequence homology from a curated list of PFam32 protein
336 sequences (see methods).

337 Applying this method to each strain, we created a comprehensive map of plasmids
338 across *Bbss* strains (Figure 4A-B). While a few plasmids are found more broadly, distinct
339 genotypes and WGS groups contain unique constellations of plasmids. Several plasmids,
340 including cp26, lp54, lp36, lp25, lp28-4, lp28-3 are found in nearly all isolates (Figure 4A-B) and
341 others such as cp32-7, cp32-5, cp32-6, cp32-9, and cp32-3 are found in most strains. Other
342 plasmids were more variable and only found in certain genotypes. OspC type A strains
343 possessed a distinct plasmid profile, containing lp56 and a unique version of lp28-1 (marked by
344 the lp28-1 PFam32 as well as a previously-annotated “orphan” PFam32 sequence, BB_F13.
345 When found in isolation, BB_F13 defines an lp28-11 plasmid [51], so is annotated as such,
346 although in many cases it may signify a subtype of lp28-1 rather than an entirely new plasmid
347 (especially OspC type A isolates whose reference is likely similar to the B31 reference[9,10]).
348 Based on PFam32 sequences, WGS A strains also contained lp28-2 and most also contained
349 lp38. OspC type K strains also contained a relatively homogenous subset of plasmids including
350 lp21, lp28-5, lp28-6, cp32-12. WGS-A/ RST1 genotypes were the least heterogeneous with
351 respect to plasmid diversity and OspC type, whereas WGS-B and WGS-C groups (RST2 and
352 RST3) were more diverse, although the subset of RST2 strains consisting of OspC type K
353 isolates was also relatively homogenous. Curiously, lp28-9 was found only in Slovenian RST1
354 isolates (Figure 4), the majority of which were OspC type B (Figure 1); cp32-12, cp32-9, and
355 cp32-1 were also found more commonly in Slovenian isolates.

356 Many plasmids (e.g. lp28-1, lp28-2, lp38 and numerous others) were found in multiple
357 distinct branches of the phylogenetic tree suggesting a complex inheritance pattern of
358 polyphyletic loss and/or recombination. This is consistent with the previously observed
359 reassortment between core genome elements and accessory genome elements (Figure 2D)
360 and genetic markers such as OspC (Figure 2H). For example, OspC types B and N both
361 contained lp28-8, whereas OspC type K genotype is most closely correlated with the lp21, lp28-
362 5 and cp32-12 pattern. lp56 is associated with OspC type A and OspC type I.

363 Specific plasmids showed significant associations with dissemination. The presence of
364 lp28-1 was associated with dissemination (OR 1.9, $p = 0.01$, Fisher's exact test), as was cp32-
365 11 (OR 1.9, $p = 0.01$) and cp32-4 (OR 2.0, $p = 0.01$) (Figure 4C-D, Supplemental Table 3). The
366 lp38 plasmid is present in roughly half of US isolates but absent in all Slovenian isolates and
367 demonstrated a trend toward being associated with dissemination (OR 1.6, $p = 0.05$).

368 To confirm the accuracy of these plasmid differences across genotype, we also
369 constructed a map of plasmid occupancy across strains by an alternate approach. We aligned
370 contigs from assembled genomes to the B31 reference sequence and annotated a plasmid as
371 "present" if the assembled contigs covered a majority of the reference plasmid sequence (Figure
372 S5A-C). Only plasmids present in the B31 reference genome were considered in this analysis.
373 These results were qualitatively similar to those obtained using the PFam32 sequences (Figure
374 S5, Supplemental Table 4) confirming that cp26, lp54, lp17, lp28-3, lp28-4 and lp36 were
375 present in nearly all strains whereas other plasmids were more variable.

376 Together, these analyses reveal a core set of plasmids present across *Bbss* strains as
377 well as strain-variable plasmids that are associated with distinct geographic and clinical features
378 (i.e., propensity to disseminate) of *Bbss*, suggesting that they contain individual genetic
379 elements that may underlie distinct disease phenotypes.

380

381 *Strain variation in core, accessory, and surface lipoproteome*

382 In an effort to implicate individual genetic elements in dissemination, the core and accessory
383 genome elements were identified in each of the sequenced isolates and all ORFs in the *de novo*
384 assemblies were annotated and clustered using BLAST, splitting clusters whose BLAST
385 homology was < 80% (Figure 5). Plotting the presence or absence of a given core or accessory
386 genome element adjacent to each isolate in the phylogeny reveals consistent patterns of ORF
387 presence/absence across closely related groups of isolates. Each of the genomic groups
388 contained unique clusters of ORFs in the accessory genome (Figure 5). The accessory genome
389 phylogenetic tree (Figure 2D, right) provided an alternative and more natural clustering of
390 accessory genome elements and PFam32 sequences (Figure S6A-B).

391 The most invasive genotype (WGS A) was associated with the largest pan-genome,
392 whereas the less invasive groups (WGS Group B and C) were associated with smaller genomes
393 (Figure 3A,B). Although many genes do not have a known function, we prioritized surface-
394 expressed lipoproteins (Figure 6) for further analysis because of their important roles in Lyme
395 disease pathogenesis and immunity (reviewed in [1,55]). We focused on the subset of all
396 lipoprotein ORFs demonstrated to be located on the surface of the spirochete [56] and divided
397 them into core (Figure 6A) and strain-variable (Figure 6B). The *Bbss* core lipoproteome (Figure
398 6A) consists of approximately 45 surface lipoprotein groups that are present in almost every
399 isolate. These include OspA and B, complement regulator acquiring surface proteins
400 (CRASPS), as well as several other lipoproteins whose functions are less well-understood. The
401 accessory lipoproteome (Figure 6B) consists of approximately 100 lipoprotein groups that are
402 strain-variable. These include lipoproteins found in only subsets of isolates, such as BB_A69
403 and BB_E31, and others, such as Decorin binding protein A (BB_A24) and OspC (BB_B19),

404 which were found in almost every isolate but broken into separate ortholog groups because of
405 extensive allelic diversity. Strain-specific clusters were also present in major gene families of
406 Erps[57,58] (Figure S7A) and Mlps[59,60] (Figure S7B). Larger numbers of these multi-gene
407 family members were found in more invasive WGS groups (A and C) (Figure 6C). The number
408 of lipoproteins in a given isolate was associated with the probability of dissemination ($\beta_1 = 0.037$
409 ± 0.017 , $p = 0.03$, logistic regression, Figure 7D). A stronger effect was seen for Erps ($\beta_1 =$
410 0.087 ± 0.053 , logistic regression, Figure 7D) with a trend toward significance ($p = 0.1$). In
411 contrast, the total number of ORFs and the number of Mlp alleles were not significant in logistic
412 regression models ($p = 0.45$ and $p=0.38$, respectively, Figure 7D). Aggregating mean effects by
413 OspC types (Figure S7E) showed similar trends.

414 Several lipoprotein groups, such as BBK32, BBK07, and BBK52 were found in almost all
415 strains, but were not found in a subset of closely related genotypes. Notably, CspZ (BBH_06)
416 and two other lipoproteins encoded on lp28-3, BB_H37 and BB_H32, were lost in two divergent
417 subsets of Slovenian isolates (Figure 6A), suggesting multiple independent loss events in
418 evolutionary history. Interestingly, these two subsets were either WGS-A or WGS-B.2, strains
419 with the greatest and least probability of dissemination (Figure S3). The increased frequency of
420 loss of lp28-3 in Slovenian isolates implies that this plasmid is likely non-essential for human
421 infection. Moreover, this finding suggests that the selective forces acting on lp28-3 may differ in
422 Europe and the US.

423 Many genes had evidence of recurrent loss or gain. For example, one cluster that shows
424 this pattern in Figure 5B contains the lipoproteins BB_J45, BB_J34, and BB_J36 along with 12
425 other genes annotated on the lp38 in B31, suggesting that these lipoproteins had been lost or
426 gained multiple times in the evolutionary tree as a part of a pattern that involved most or all of
427 lp38.

428

429 *Associations between Accessory Genome Elements, Genotype, and Dissemination*

430 The genetic basis of the phenotypic differences between these strains most likely includes
431 nucleotide-level variation in chromosomal and plasmid DNA as well as variation in gene
432 presence or absence in the accessory genome (which is primarily plasmid-borne). While it is not
433 feasible to resolve these associations definitively in this study, we attempted to identify
434 preliminary ORF-level associations by clustering ORFs according to homology using Roary [44].
435 We then applied linear mixed models genome-wide study approaches to identify ortholog
436 groups associated with disseminated infection (Figure 7A-B). We used the approach of Earle et.
437 al [61] to distinguish “locus” and “lineage” effects by identifying lineages that were associated
438 with a phenotype.

439 Two lineages, defined by principal components of the distance matrix between isolates,
440 were significantly associated with the phenotype of dissemination (MDS10, $p = 0.02$, Wald’s
441 test), and a second component was borderline associated (MDS8, $p = 0.08$, Wald’s test). The
442 results of all analyses are reported in Supplemental Table 5 and lipoprotein-specific analyses in
443 Supplemental Table 6. In ancestry-adjusted association logistic regression analysis in which
444 principal components were included as covariates [62], only a handful of loci were associated
445 with phenotype, and their genomic position was distributed throughout the genome with no
446 strong spatial pattern (Figure 7B). The uncorrected association statistics showed somewhat
447 stronger correlations that were concentrated in the plasmids (Figure 7A).

448 We also used the pan-genome association approach to identify associations between
449 ortholog groups and single-locus genetic markers. Single-locus genetic markers were strongly
450 linked to genetic variation in ORFs, particularly among plasmids (Figure 8; Supplemental Table
451 7 for OspC Type A; Supplemental Table 8 for OspC Type K; Supplemental Table 9 for RST1).

452 The strongest effects were seen among surface-exposed lipoproteins [56] (Figure S8).
453 Together, these results, along with those of Figure 6, demonstrate that individual *Bbss*
454 genotypes represent a tightly-linked set of genetic variation that confers a distinct surface
455 lipoproteome.

456 Due to the structural patterns of genetic diversity in *Bbss*, ORFs associated with
457 phenotype without ancestry correction (Figures 6D and Figure 7A) should not be ignored. Due
458 to the near-complete linkage (e.g. Figure 8) between genetic elements in the accessory
459 genome, individual loci with strong, causal effects on a given phenotype may not be separable
460 from their set of linked variants, i.e. their background lineage. OspC type A strains, which are
461 included among the strains with the highest rates of dissemination in this study (Figure S4) and
462 as reported previously [3,4], and which have been linked to more severe symptoms of Lyme
463 disease [3] (Figure S4C), are strongly associated with a set of approximately 75 loci (OR > 50)
464 including a DbpA ortholog group (OR 4964, $p = 1.9 \times 10^{-48}$, likelihood ratio test), an OspC
465 ortholog group (OR 2951, $p = 1.9 \times 10^{-48}$, likelihood ratio test), and BB_H26 (OR 2186, $p = 4.9 \times$
466 10^{-38} , likelihood ratio test). These and other linked alleles were strongly correlated with one
467 another ($r = 0.94$, $p < 2.2 \times 10^{-16}$ for DbpA/group1807 and OspC/group1021; $r = 0.85$, $p < 2.2 \times$
468 10^{-16} for DbpA/group and BB_H26). In many cases this linkage is physical due to presence on
469 the same replicon (e.g. the BB_J alleles on lp38), strongly linked allelic groups may also be
470 present on distinct replicons (e.g. DbpA on lp54 and OspC on cp26). While the strong
471 correlations between individual alleles make it difficult to separate the statistical effects of
472 individual alleles, such correlations are also the characteristic and defining feature of *Bbss*
473 lineages.

474

475 **Discussion:**

476 The sequencing and analysis of 299 human clinical isolates of *Bbss* that we report here
477 provides a previously unavailable level of resolution into the *Bbss* genetic and geographic
478 diversity of *Bbss* strains causing Lyme disease. Our collection of WGS assemblies from these
479 isolates—which were collected across distinct geographic regions, and which were linked to
480 certain clinical manifestations, and systematically typed with RST, OspC, and MLST—lays a
481 foundation for further research and advances our understanding of Lyme disease in several
482 ways.

483 First, our results confirm and extend previous findings on the microbial genetic basis of
484 disease manifestations in humans. Prior studies have identified genetic markers and correlated
485 their presence with specific clinical findings [1,3,5,6,8,26,27,29–32], but the relationships among
486 these markers and specific *Bbss* genes that cause phenotypic differences had not yet been
487 studied due to limitations of existing typing systems and a lack of human isolates. Along with the
488 novel genetic diversity uncovered by sequencing additional clinical isolates, the statistical
489 evidence linking genetic elements to dissemination and geography that was observed in this
490 study will be useful in prioritizing candidate genes and/or loci for further experimental evaluation.
491 For example, we confirm here previous findings that WGS A / RST1 — particularly the subtype
492 defined by OspC type A — is genetically distinct [27,63–65], and we identify certain genetic
493 alterations associated with this lineage, including having a larger number of ORFs than other
494 lineages. These ORFs are found on a strain-specific constellation of plasmids, including lp28-1
495 and lp56. This is consistent with previous findings that have linked the presence of lp28-1 to
496 infectivity in mouse models [66–69]. Importantly, these results extend previous findings which
497 showed that RST1 OspC type A strains are associated with more severe Lyme disease [3], by
498 identifying candidate plasmids lp28-1 and lp56 as potential genetic factors associated with

499 greater virulence of these *Bb* genotypes in patients. We show that this association, derived from
500 mouse models, extends to humans.

501 Second, the microbial genetic association studies presented here begin to resolve the
502 individual genetic elements underlying certain human phenotypes of Lyme disease. Using two
503 different methods to infer the presence or absence of plasmids, we provide the first plasmid
504 presence / absence maps of a large collection of human clinical isolates. Integrating this
505 information with associations at the level of individual ORFs provides a clearer view of the
506 potential determinants of distinct phenotypes. While we cannot yet resolve the causative loci on
507 lp28-1 or lp56 that enhance the pathogenicity of OspC type A strains, we highlight candidate loci
508 and quantify the statistical evidence for each locus considered. ORFs in these plasmids such as
509 BB_Q67 (which encodes a restriction enzyme modification system [70,71]), BB_Q09, BB_Q05,
510 BB_Q06, BB_Q07, BB_J31, BB_J41 and others (Supplemental Table 8) are tightly linked to the
511 OspC type A genotype and are candidates for further experimental study.

512 In addition, our sub-analysis of surface-exposed lipoprotein sequences (Figures 6A and
513 6B) may also be useful for experimental follow-up given the importance of surface lipoproteins
514 for immunity, pathogenesis, and *Bb*ss-host interactions (reviewed in [1,55]). Particular alleles of
515 DbpA (BB_A24), and specific members of the Erp (BB_M38, BB_L39) and Mlp (BB_Q35)
516 (supplemental data file 2, Figures 6C and 6D) families are associated with dissemination and
517 represent potential candidates for evaluation in follow-up studies. Both the specific list of ORFs
518 strongly associated with OspC type A and the more general pattern of variation across strains
519 provides clues into enhanced virulence. Among those ORF groups associated with the OspC
520 genotype, allelic variants of DpbA have been shown to promote dissemination and alter tissue
521 tropism in a mouse model of Lyme disease [72]. Multiple genes in linked blocks probably
522 contribute to pathogenesis. For example, In OspC type A strains, DbpA is strongly linked to

523 OspC type A. Allelic variation in OspC alters binding to extracellular matrix components,
524 promotes joint invasion, and modulates joint colonization[73]; OspC has also been shown to
525 promote resistance in serum killing assays [74], and its role in causing infection can be, under
526 certain circumstances, partially complemented by other surface lipoproteins [75,76].

527 Our data suggest that copy number among multi-copy gene families may be linked to
528 dissemination. Given that Erps are divided into three families that each bind to distinct host
529 components (extracellular matrix, complement component, or complement regulatory protein)
530 [58,77–80]; it is possible that the strain-variable clusters of Erps (Figure S7B, Figure S7D-E)
531 may influence clinical manifestations by modulating strain-specific properties of tissue adhesion
532 or resistance to complement-mediated killing of spirochetes. The functions of Mlp proteins and
533 many other strain-variable lipoproteins are still not well understood. The statistically-significant
534 relationship between lipoprotein number and probability of dissemination and the borderline-
535 significant relationships for copy number of Erps and Mlps (Figure S7D-E) suggest that varying
536 the amount and diversity of linked clusters of surface lipoproteins—which, individually or in
537 combination, may promote survival in the presence of immune defenses, binding to mammalian
538 host tissues and other pathogenic mechanisms— may be a general mechanism for strain-
539 specific virulence of *Bbss*.

540 Using unadjusted, univariate associate models, virtually all dissemination-associated
541 genes were found on plasmids. However, after correction for spirochete genetic structure due to
542 lineage, only weak locus-specific associations were observed. The block patterns of Figures 5
543 and 6 demonstrate why this is the case. Genes are inherited in blocks; the inheritance pattern of
544 genes within these blocks is strongly correlated such that only infrequently are genes from
545 within a block found in isolates that are outside the block. This pattern is also seen in plasmids,
546 and plasmids are a natural mechanism for this pattern of inheritance. An important

547 consequence of this finding is that it may not be possible to resolve individual loci beyond
548 correlated blocks of genes simply by increasing the number of samples or other methods to
549 improve statistical power because the near-complete correlation between individual loci makes
550 it statistically difficult to distinguish the individual effects among correlated genes. Thus, beyond
551 identifying genomic elements or groups of correlated genes associated with a phenotype,
552 further fine mapping will require biological experiments with reverse genetic tools. The results
553 shown in Figure 6 and 7, and Supplemental Data File 3 are helpful in narrowing down the
554 candidate loci and genetic elements that may predispose to or protect from dissemination.

555 Third, our analysis highlights how evolutionary history, geography, and differences in
556 strain genetic diversity interact in complex ways to contribute to clinical heterogeneity in Lyme
557 disease. In the context of known associations between genotype and clinical disease, the
558 difference in genetic markers across geographic areas may help explain why some clinical
559 phenotypes are more common in certain geographic locations. For example, Lyme arthritis is
560 more common in the US compared to Europe, probably because the infection in the US is due
561 predominantly to *Bbss* strains which are more arthritogenic [81]). *OspC* type A strains appear to
562 be more common among patients in the US Northeast [26,27]. The intermixing of WGS groups
563 B and C in RST types 2 and 3 has not been a major issue in practice because the phenotypes
564 (for example, the relative rate of dissemination) of those groups appear more similar than the
565 genomically and phenotypically divergent RST1 / WGS A group. Similarly, *OspC* genotyping
566 has its limitations. The large number of *OspC* types (at least 30) makes phenotypic associations
567 with specific *OspC* genotypes challenging. More importantly, the discordance between *OspC*
568 sequences and whole-genome phylogenies—a discrepancy observed since the earliest *OspC*
569 sequences were published [82] and likely related to the fact that the *OspC* locus is a known
570 recombination hotspot on *cp26* [83]—may make *OspC* unreliable as a genetic marker of

571 phenotypic traits. In this regard, WGS serves as a gold standard against which other typing
572 methods can be compared, facilitated here by our sequenced and fully-typed set of isolates.

573 WGS also offers new insight into evolutionary history and population divergence of *Bbss*.
574 Estimation of divergence times suggests a remote (at least hundreds of thousands of years)
575 origin for human infectious *Bbss*. The similarity in TMRCA estimates for samples from Slovenia,
576 the US Northeast, and the US Midwest indicate that the common ancestry for sequences
577 currently circulating in these populations is also remote; however, the strong lineage structure
578 and history of multiple exchanges suggests that the local history of distinct lineages is also
579 complex likely with multiple inter-region migration events. The consistent directional differences
580 in ORF number by region also suggest that adaptive evolution to local environments has
581 occurred, exploiting mechanisms of gene loss/gain on plasmids.

582 This report has several limitations. First, plasmids pose a unique challenge for assembly
583 and annotation [10,12]. As others have shown [13], complete plasmid assembly with short read
584 sequences is not possible. We devised two bioinformatic methods to overcome these changes
585 and infer plasmid presence/absence from short read sequencing, but neither is perfect. Our
586 PFam32 analysis is limited by an uncertainty as to which gene sequences are contained on the
587 plasmid associated with the PFam32 sequence. A complementary analysis based on the B31
588 reference sequence relies on a high-quality pre-existing assembly but cannot account for
589 genes/plasmids absent from the B31 reference. We also cannot exclude the possibility of
590 plasmid loss during culture, but isolates were passaged fewer than five times to minimize this
591 possibility.

592 Second, there are limitations due to analysis of isolates collected over time by different
593 groups at different sites. In particular, we may underestimate dissemination because an
594 assessment of spirochetemia (blood PCR or blood culture) was only available for 70.9% of

595 isolates (supplemental data file 3) and the absence of positive culture or blood PCR from a
596 single time point does not rule out the possibility that dissemination from the initial skin lesion
597 may have occurred or may occur at a later time in untreated patients.

598 Third, there are statistical limitations related to the *Bbss* genome and study size. Models
599 that naively correlate a given gene with the phenotype of interest will produce spurious
600 associations due to the confounding effect of lineage and may overstate the effect from single
601 loci, a problem which is well known in human genome-wide association studies [84]. Corrections
602 for lineage and population structure are often applied to human [85,86] and bacterial [61,62]
603 association studies. However, *B. burgdorferi* underscores the challenges to these approaches,
604 both because lineages appear to be *defined* by the exchange of blocks of genes and because
605 the coarse tree structure differs for the core and accessory genomes, implying that a single
606 similarity measure to capture the pairwise dissimilarity between strains may not be adequate.
607 Larger studies with more isolates, statistical methods that incorporate the joint distribution
608 between genetic markers, and plasmid assemblies finished by long read sequencing are
609 required as a next step. The present study includes isolates collected by different investigators
610 over the past 30 years. Due to the logistical complexity and cost of collecting *Bbss* isolates from
611 patients in clinical studies, substantially larger studies of *Bbss* from patients may not be feasible
612 in the near term; however, long-read sequencing approaches have improved in accuracy,
613 availability, and cost, making finishing the genomes of existing isolates a logical next step.

614 Taken together, our results indicate that each *Bbss* genotype represents a tightly-linked
615 constellation of strain-specific variation that occurs primarily in plasmids, much of it involving
616 surface-exposed lipoproteins. OspC type A strains—with their enlarged pan-genome, distinct
617 set of plasmids, including lp28-1 and lp56, and variants of many surface lipoproteins, particularly
618 a unique subtype of DbpA—represent the most dramatic example of this genetic signature

619 associated with distinct phenotypes of Lyme disease in humans. Nevertheless, the pattern is
620 generalizable across genotypes and, given the strong linkage between microbial genotype and
621 phenotype for *Bbsl*, and similarities in genetic structure among *Bbsl* genomes, is likely true
622 broadly across all Lyme disease agents (*Bbsl*).

623

624 **Acknowledgments:**

625 This work was supported by a Doris Duke Charitable Foundation Physician Scientist Fellowship
626 (2019123 to J.E.L), the National Institute of Allergy and Infectious Diseases (K99/R00148604 to
627 J.E.L, U19AI110818 and U01 AI151812 to P.C.S.; R01AI045801 to I.S., and R21AI144916 to
628 K.S.), the National Institute of Arthritis and Musculoskeletal and Skin Diseases (R01AR41511 to
629 I.S. and K01AR062098 to K.S.), the Bay Area Lyme Foundation (to P.C.S. and J.E.L.), the
630 Howard Hughes Medical Institute (P.C.S.), the Arthritis Foundation Fellowship (to K.S.), and the
631 Slovenian Research Agency (P3-0296, J3-1744, and J3-8195 to F.S.).

632

633 **Declaration of interests:**

634 P.C.S. is a co-founder of, shareholder in, and consultant to Sherlock Biosciences and Delve Bio,
635 as well as a board member of and shareholder in Danaher Corporation. K.S. served as a
636 consultant for T2 Biosystems, Roche, BioMerieux, and NYS Biodefense Fund, for the
637 development of a diagnostic assay in Lyme borreliosis. F.S. served on the scientific advisory
638 board for Roche on Lyme disease serological diagnostics and on the scientific advisory board
639 for Pfizer on Lyme disease vaccine, and is an unpaid member of the steering committee of the
640 ESCMID Study Group on Lyme Borreliosis/ESGBOR. J.A.B. has received research funding
641 from Analog Devices Inc., Zeus Scientific, Immunetics, Pfizer, DiaSorin and bioMerieux, and
642 has been a paid consultant to T2 Biosystems, DiaSorin, and Roche Diagnostics.

643 G.P.W. reports receiving research grants from Institute for Systems Biology, Biopeptides, Corp.,
644 and Pfizer, Inc. He has been an expert witness in malpractice cases involving Lyme disease
645 and babesiosis; and is an unpaid board member of the non-profit American Lyme Disease
646 Foundation.

647

648 **Data and code availability:**

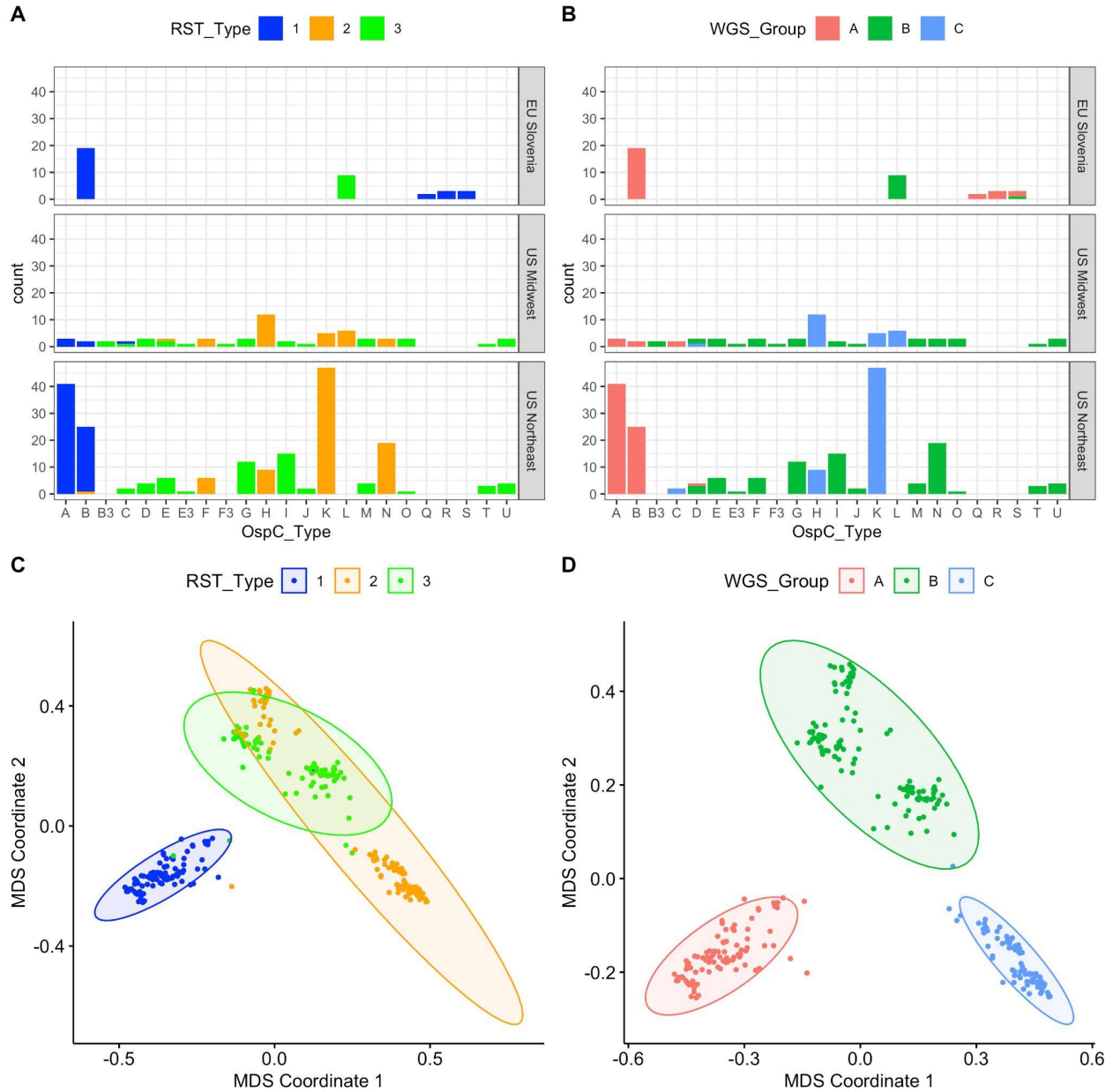
649 Genome sequences reported here have been deposited in [Genbank](#) under PRJNA923804.

650 Code is available at <https://github.com/JacobLemieux/borreliaseq>.

651

652

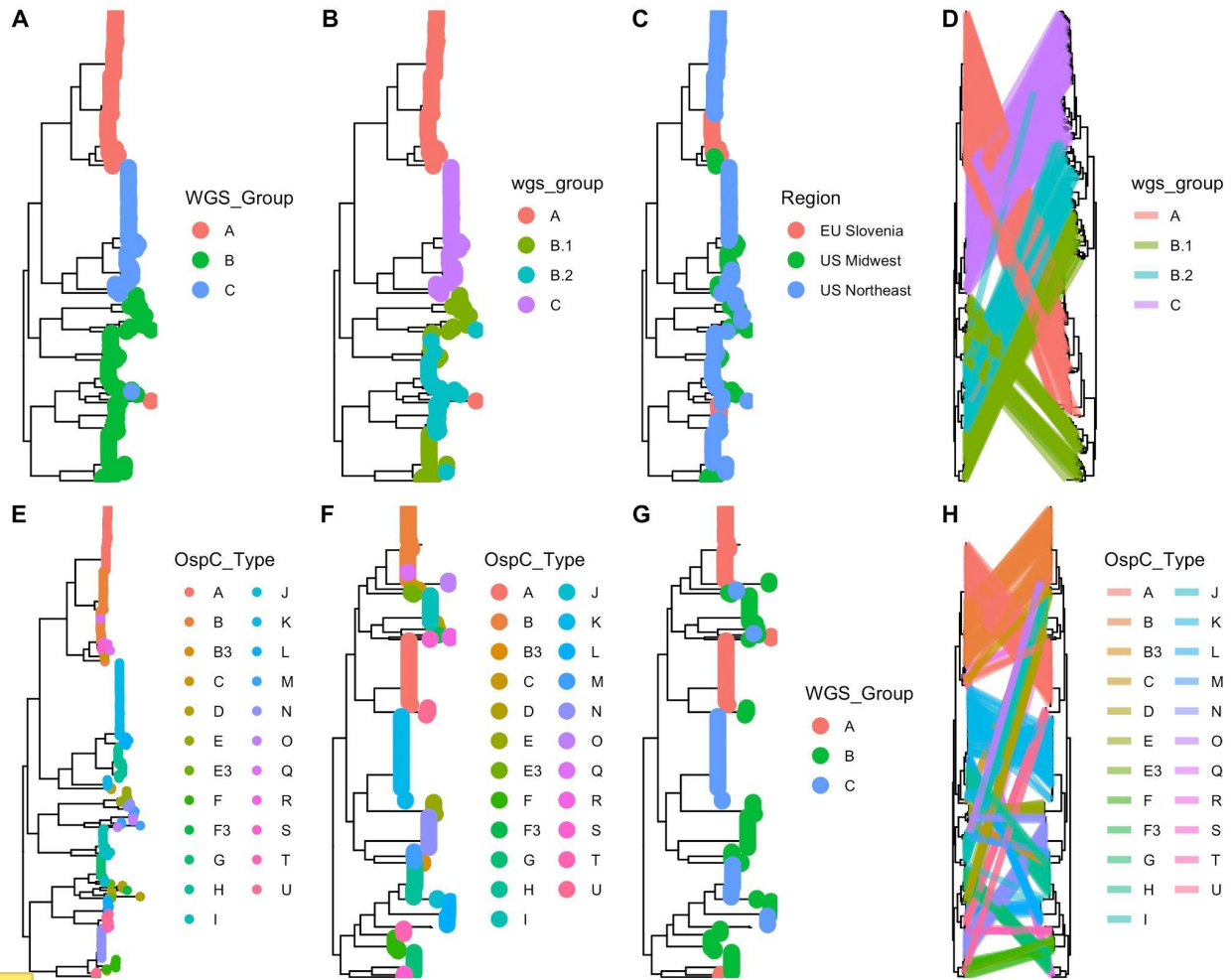
653



654
655
656
657
658
659

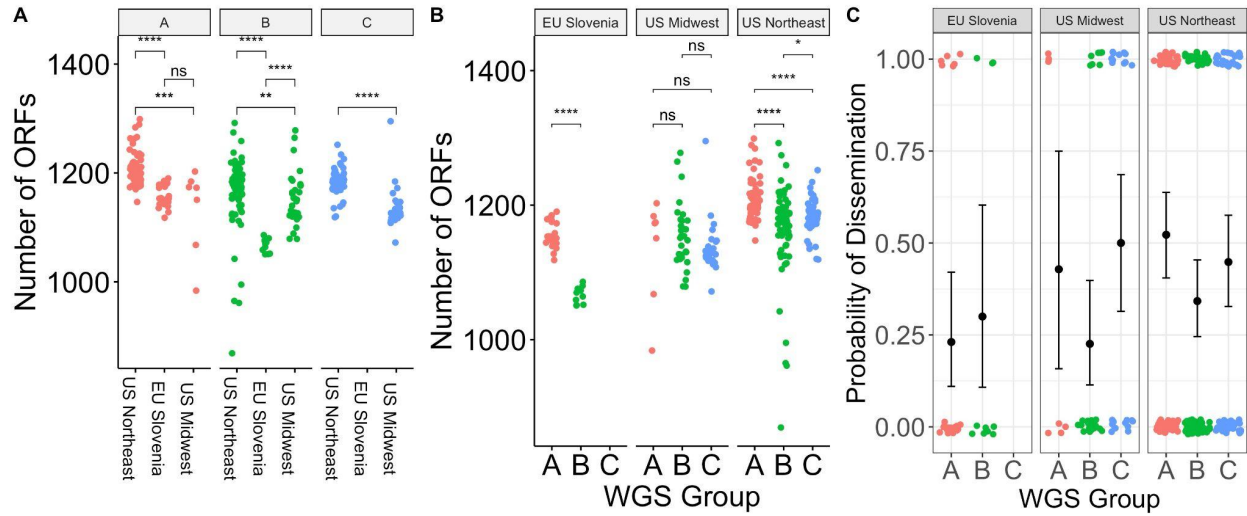
Figure 1: **A.** Counts of samples according to RST and OspC type. Top, middle, and lower panels show samples from different geographic regions. X-axis gives OspC type. Bars are colored according to RST type. **B.** Plots as in (A) but with bars colored according to the WGS group. **C.** Multidimensional scaling (MDS) of 299 *Bbss* genomes, with WGS RST type annotated. **D.** MDS of 299 *Bbss* genomes, with WGS type annotated.

660



661

662 **Figure 2: A-B.** Core genome phylogenetic tree with tips labeled by the three major WGS groups
 663 (A). **B.** Core genome phylogeny with WGS group B split into subgroups (B.1 and B.2). **C.** Core
 664 genome phylogenetic tree with tips labeled by region of collection. **D.** The core genome
 665 phylogenetic tree (left) compared to the accessory genome phylogenetic tree (right). Lines,
 666 colored by WGS groups, connect tips from identical samples. **E.** WGS tree with tips colored by
 667 OspC type. **F.** OspC tree with tips colored by OspC type. **G.** OspC tree with tips colored by
 668 WGS group. **H.** WGS tree (left) and OspC tree with identical tips connected by strain lines,
 669 colored by OspC type.



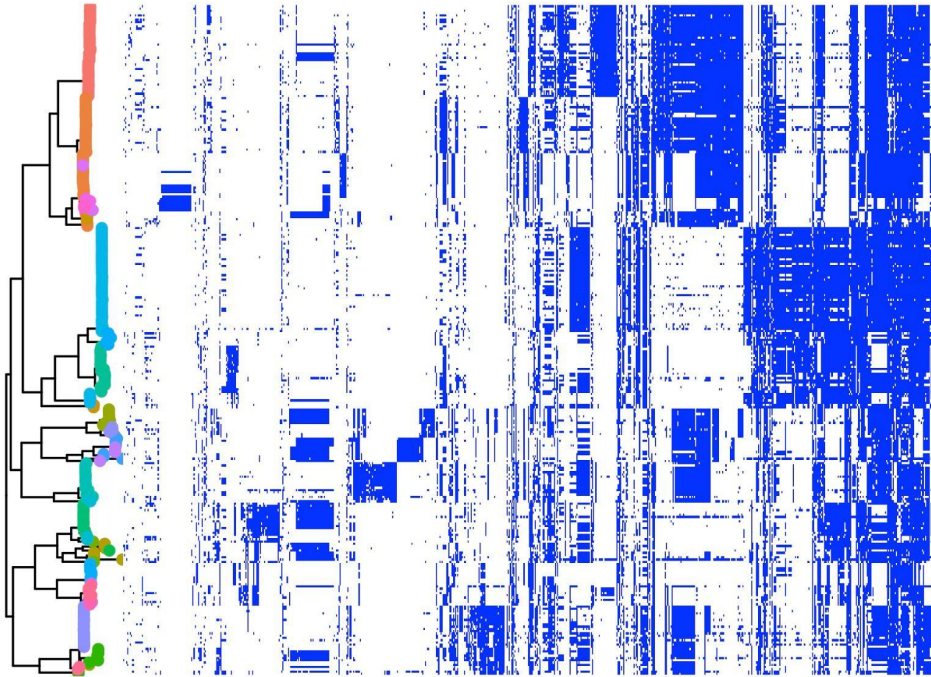
670
671
672
673
674
675
676
677

Figure 3: A. Number of ORFs by geographic region in different WGS groups. * denotes $p < 0.05$; ** denotes $p < 0.01$; *** denotes $p < 0.001$; **** denotes $p < 0.0001$; ns - not significant. **B.** Number of ORFs by WGS group in different geographic regions. **C.** Probability of dissemination by genomic group. Each point represents a sample. Points are colored by WGS group. The samples that disseminated have been plotted at $y = 1$; those that did not have been plotted at $y = 0$. Random noise has been added to the x- and y- coordinate to display the points. The mean \pm 95% binomial confidence interval is shown for each group with error bars.

689 using Fisher's exact test) and the odds ratio of dissemination for each plasmid, inferred by
690 Pfam32 sequences.

691

A



OspC_Type

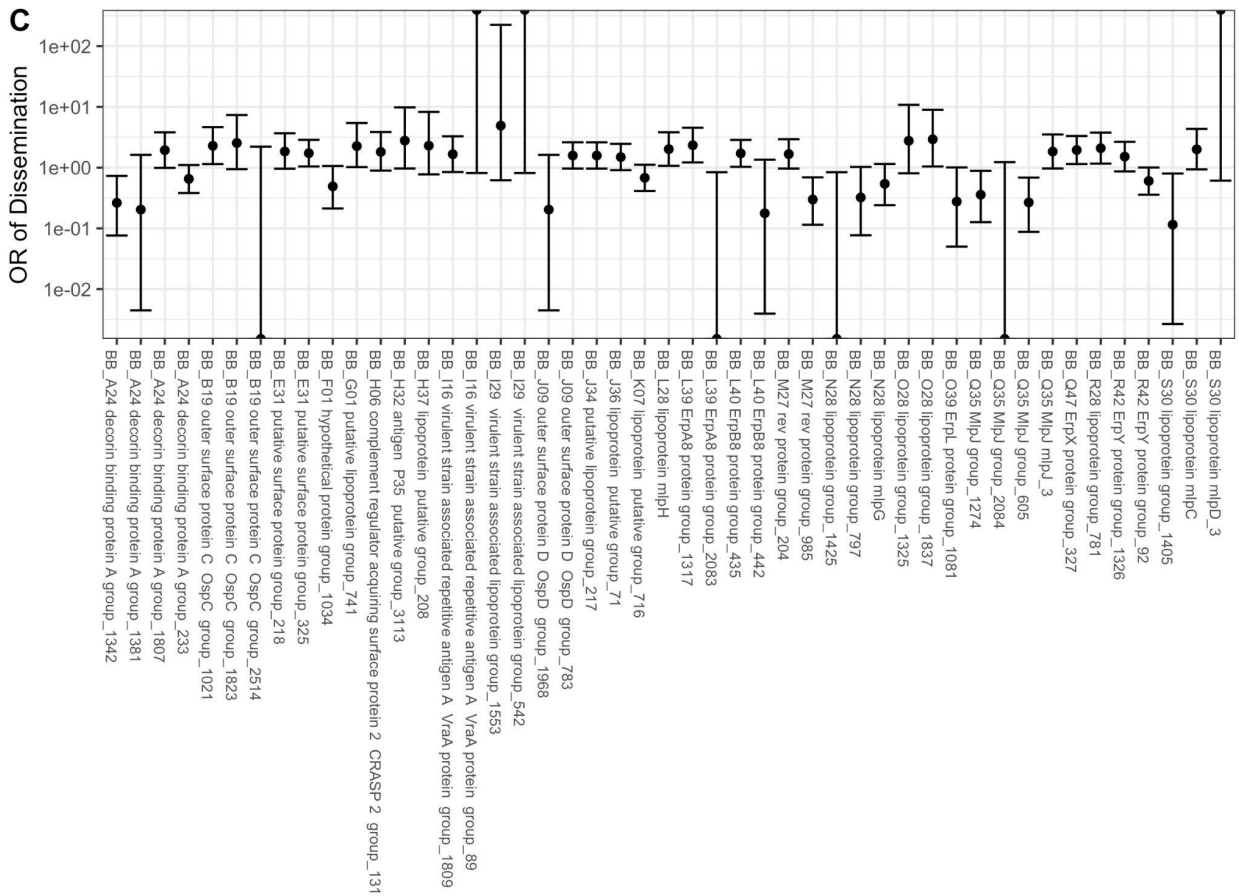
-
 A
-
 B
-
 B3
-
 C
-
 D
-
 E
-
 E3
-
 F
-
 F3
-
 G
-
 H
-
 I
-
 J
-
 K
-
 L
-
 M
-
 N
-
 O
-
 Q
-
 R
-
 S
-
 T
-
 U

ORF

-
 Present
-
 Absent

692

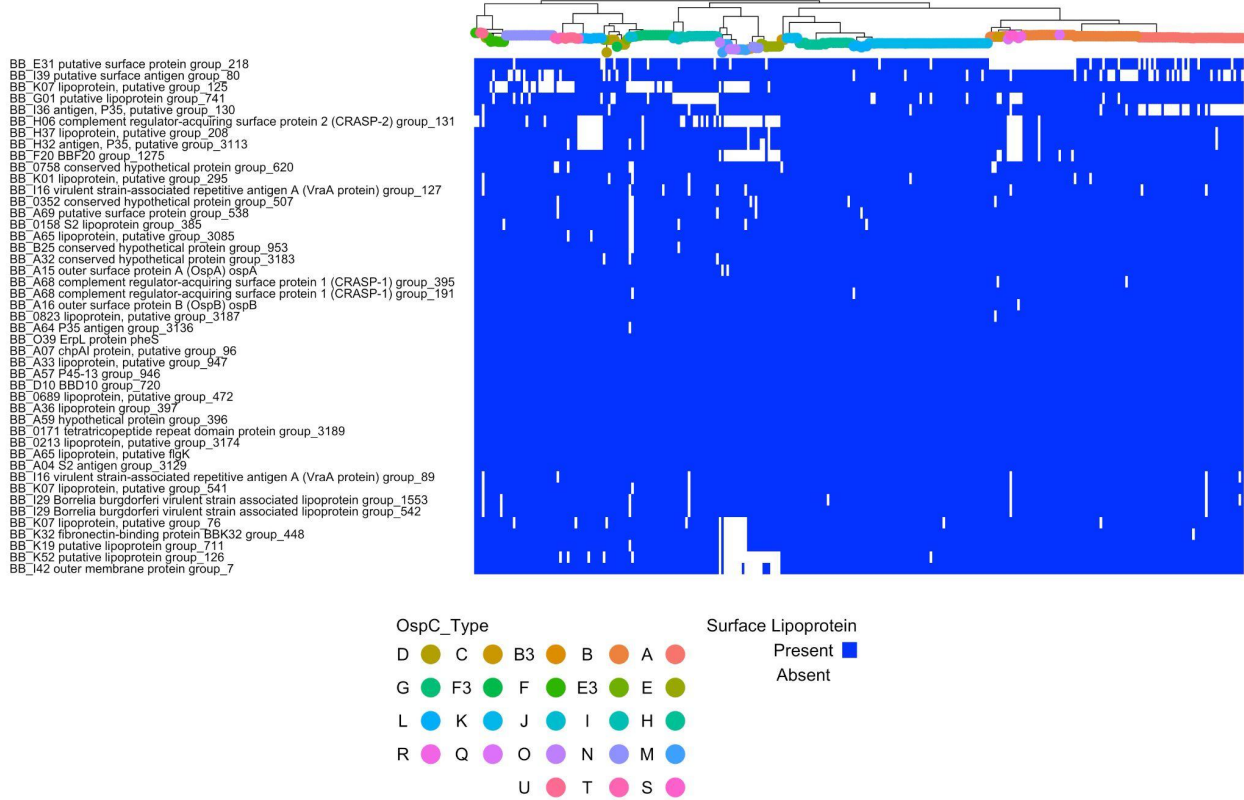
C



693

694 **Figure 5: A.** Core genome phylogeny with tips colored by OspC type. **B.** The phylogeny is
695 plotted alongside a matrix of presence (blue) or absence (white) for genes in the accessory
696 genome. The rows of the matrix are ordered by the phylogenetic tree in **A.** The columns of the
697 matrix are ordered using hierarchical clustering such that genes with similar patterns of
698 presence/absence across the sequenced isolates are grouped close together. **C.** Odds ratio
699 (OR) of dissemination and 95% confidence interval for ortholog groups encoding surface-
700 exposed lipoproteins and for which the unadjusted p-value for association with dissemination
701 (by Fisher's exact test) is < 0.15 .

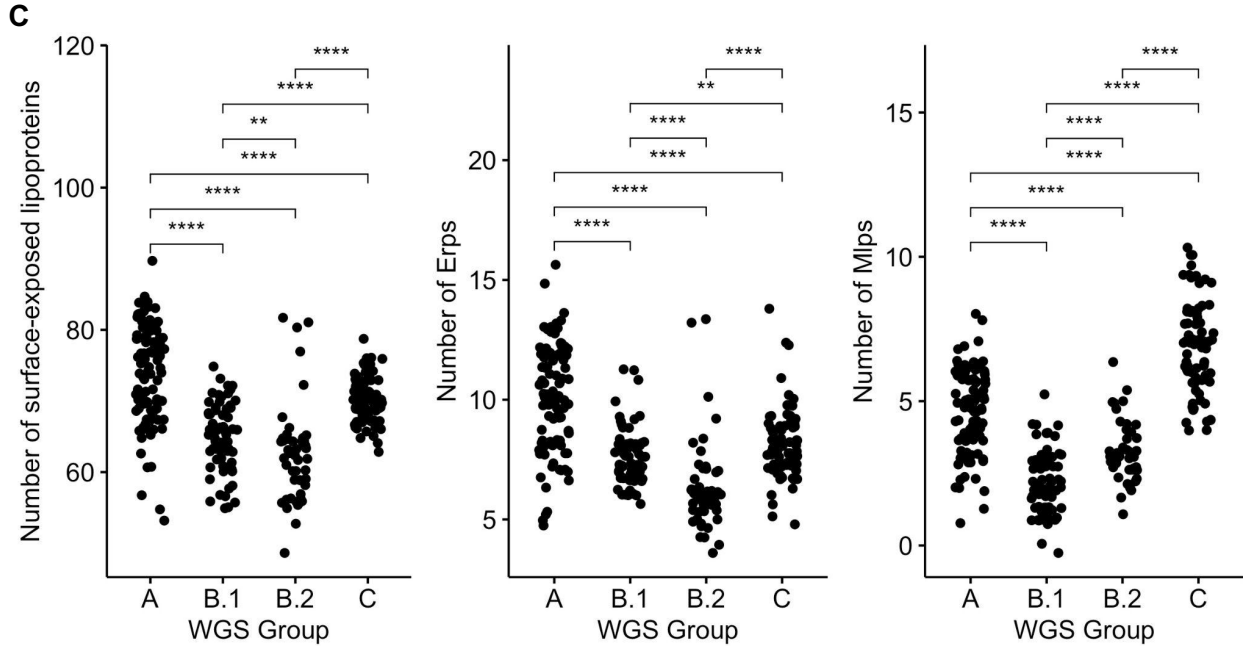
702 A



703



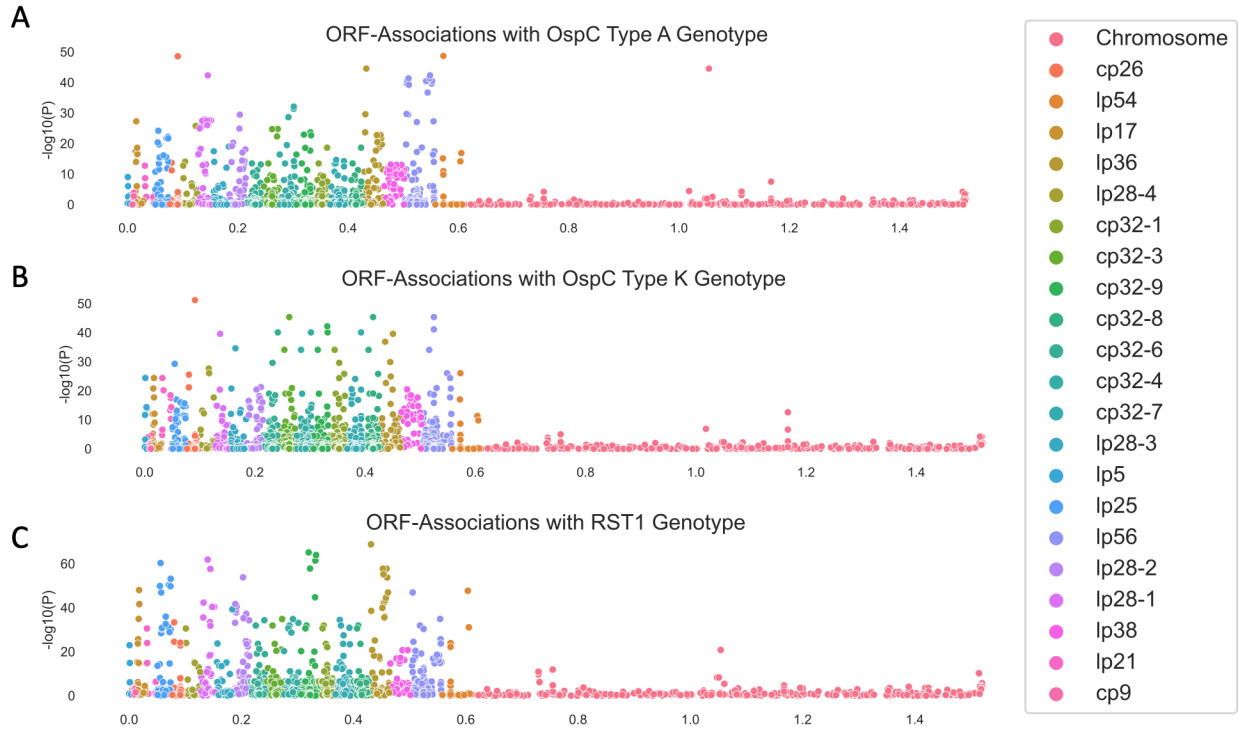
708



709

710 **Figure 6 : A.** *Bbss* core surface lipoproteome: Core genome phylogeny with tips colored by
 711 OspC type (colored according to the scheme in Figure 5) with a matrix of presence (blue) or
 712 absence (white) for surface lipoproteins. Surface-exposed lipoproteins present in at least 80% of
 713 strains were considered to be part of the core lipoproteome. **B.** *Bbss* strain-variable (accessory)
 714 surface lipoproteome: Core genome phylogeny with tips colored by OspC type (colored
 715 according to the scheme in Figure 5) with a matrix of presence (blue) or absence (white) for
 716 surface lipoproteins. Surface-exposed lipoproteins present in between 5% and 80% of strains
 717 were considered to be part of the strain-variable (accessory) lipoproteome. **C.** The number of
 718 surface-exposed lipoproteins (left panel), Erps (middle panel), and Mlps (right panel) by WGS
 719 group. ** denotes $p < 0.01$; *** denotes $p < 0.001$; **** denotes $p < 0.0001$.

723 **Figure 7:** Manhattan Plots showing the association of individual ORF ortholog groups with the
724 phenotype of dissemination. **A.** P-values from univariate logistic regression by genomic position
725 for each ORF. **B.** P-values from regression estimates that include principal components
726 distance matrix between strains. **C.** Manhattan plot showing loci associated with each lineage
727 for the lineages associated with phenotype. **D.** Odds ratios (OR) ($\exp(\beta)$) with 95%
728 confidence interval are shown for dissemination for the lineage-adjusted model. ORFs with $p <$
729 0.1 and allele frequency > 0.1 and < 0.9 are displayed.
730
731

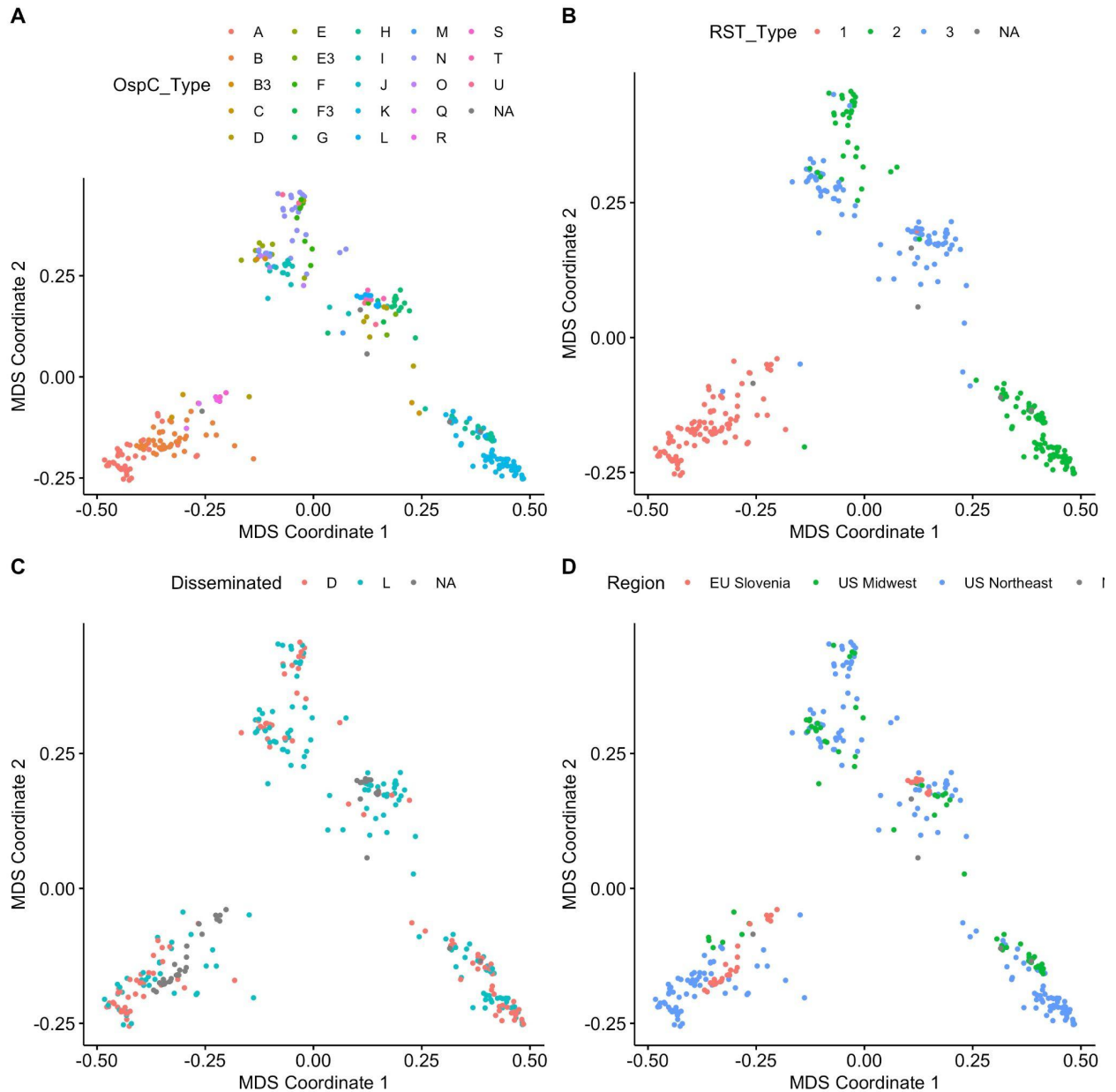


732
733
734
735
736

Figure 8: Manhattan Plots showing the association of individual ORF ortholog groups with OspC type A (panel **A**), Osp C type K (panel **B**), and RST1 (panel **C**).

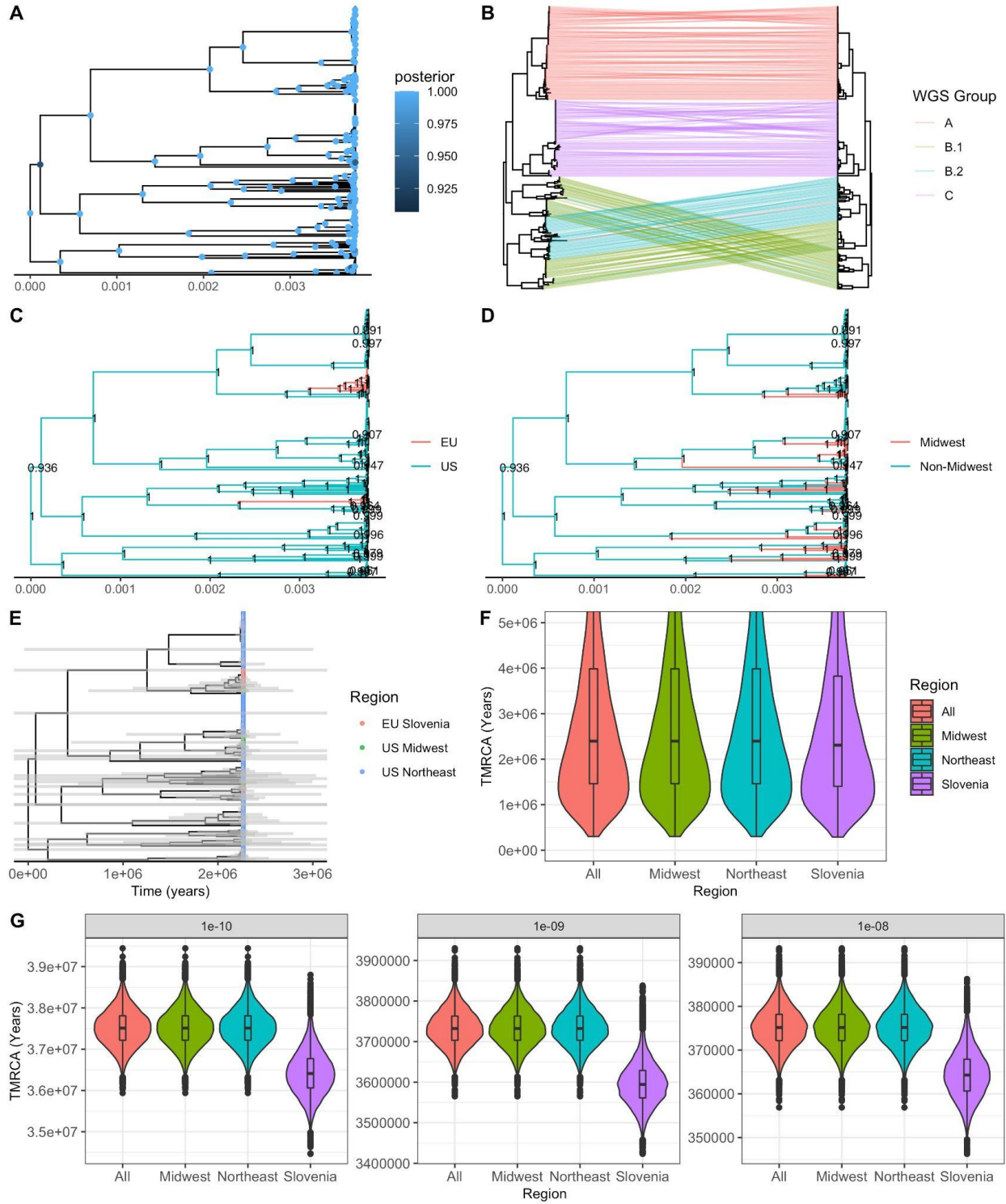
737 Supplemental Figures:

738

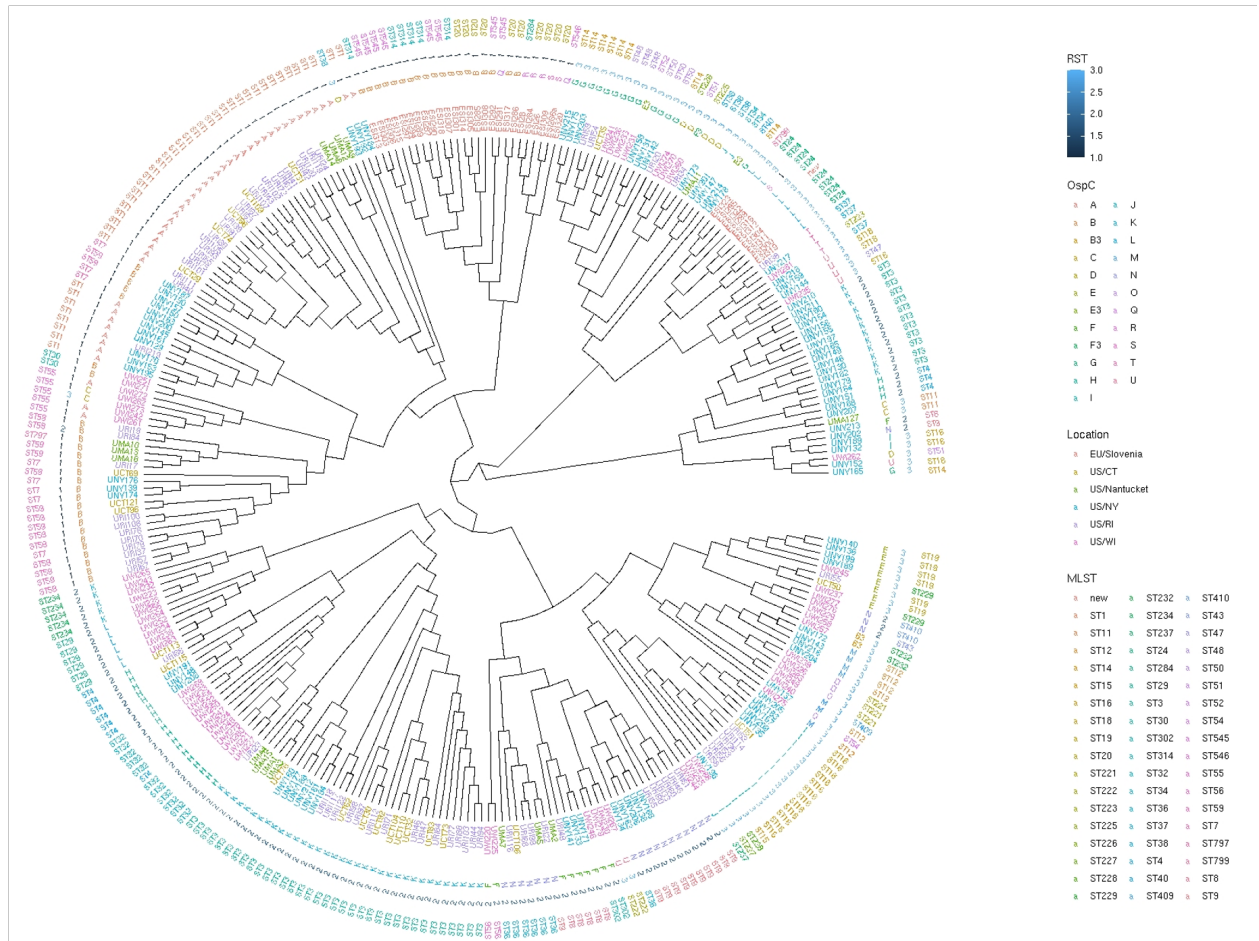


739
740
741

Supplemental Figure 1: Multidimensional scaling (MDS) reveals the population structure of US and Slovenian *Bbss* isolates.



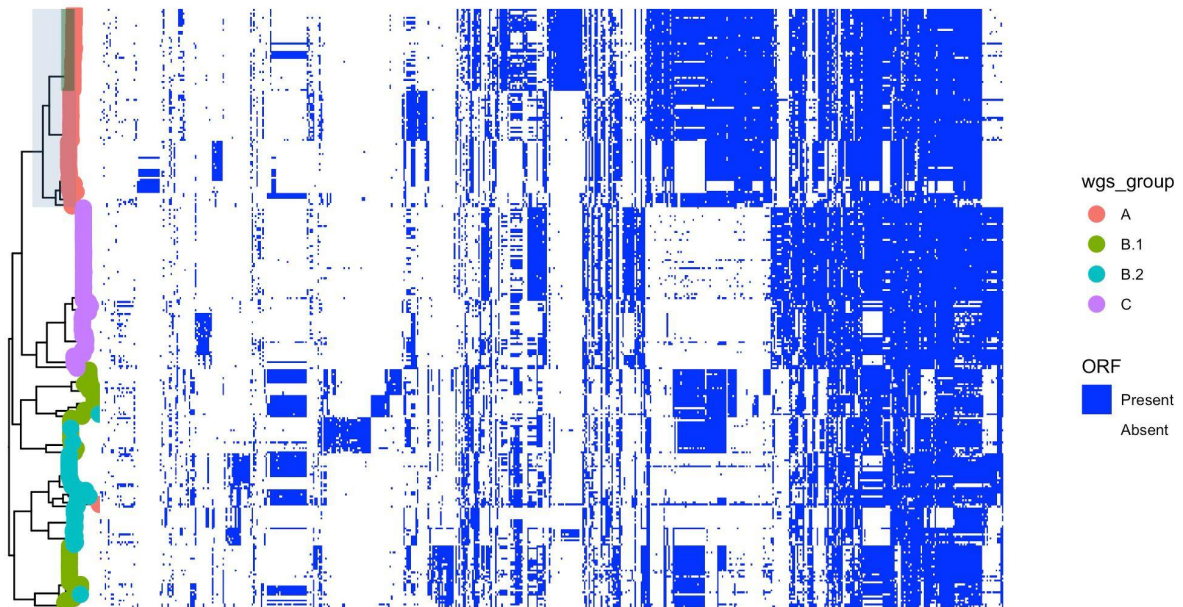
742
743



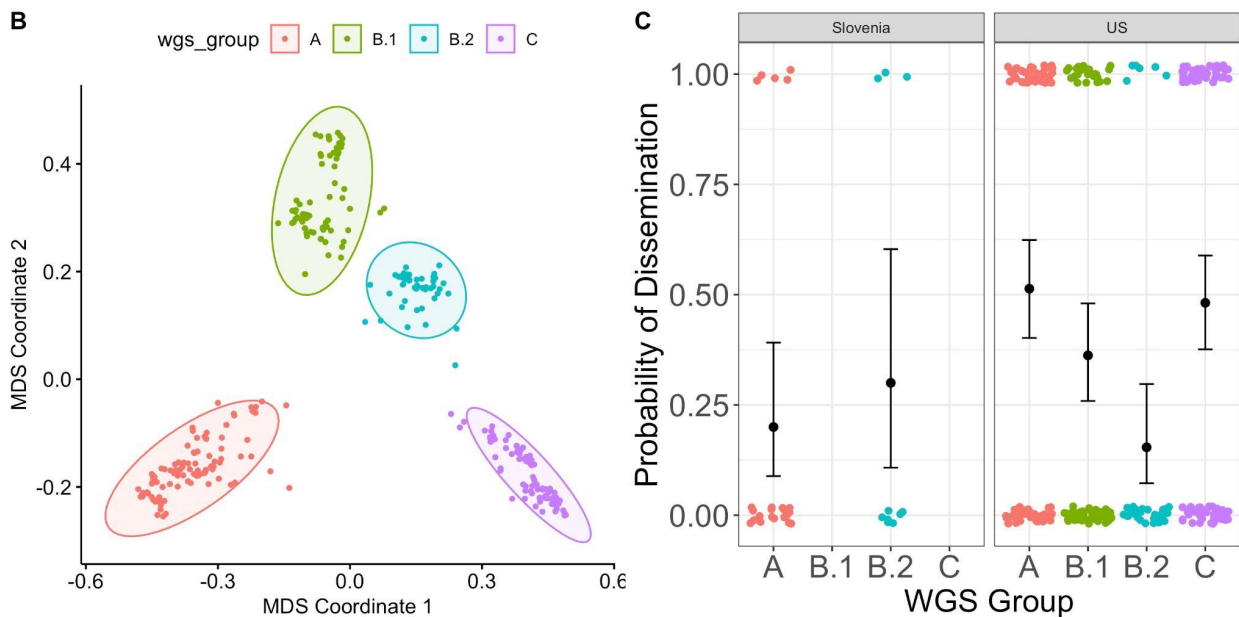
745

746 **Supplemental Figure 2: A.** Maximum clade credibility (MCC) tree. Nodes with posterior
 747 probability > 0.9 are colored. **B.** Maximum likelihood (left panel) and MCC tree, with identical
 748 tips connected with lines colored according to WGS group. **C.** MCC tree with nodes with
 749 posterior probability > 0.9 labeled. Tips from the US have been grouped and their most recent
 750 common ancestor are colored blue; all others are colored red. **D.** MCC tree with nodes with
 751 posterior probability > 0.9 labeled. Tips from outside the US Midwest have been grouped and
 752 their most recent common ancestor are colored blue; all others are colored red. **E.** Time-tree
 753 with 95% credible interval of node heights plotted as gray bars. **F.** Density of time to most recent
 754 common ancestry (TMRCA) for major subpopulations and the full sample set (root). An inset
 755 boxplot gives the median and IQR. **G.** Density of time to most recent common ancestry
 756 (TMRCA) for major subpopulations and the full sample set (root) under three different fixed-
 757 clock models with the clock rate set at 1×10^{-10} substitutions/site/yr (left panel), 1×10^{-9}
 758 substitutions/site/yr (middle panel), or 1×10^{-8} substitutions/site/yr (right panel). **H.** Core genome
 759 phylogeny of 299 whole-genome sequences. The phylogeny is shown as a cladeogram (branch
 760 length does not correspond to genetic distance). The tips are labeled with sample names. RST
 761 type, OspC type, location, and MLST type are annotated. Whole genome sequences
 762 recapitulates existing typing schemes while adding additional resolution. Geographic origin is
 763 associated with different branches of the tree. For example, Slovenian isolates cluster in two
 764 distinct branches.
 765

766 A



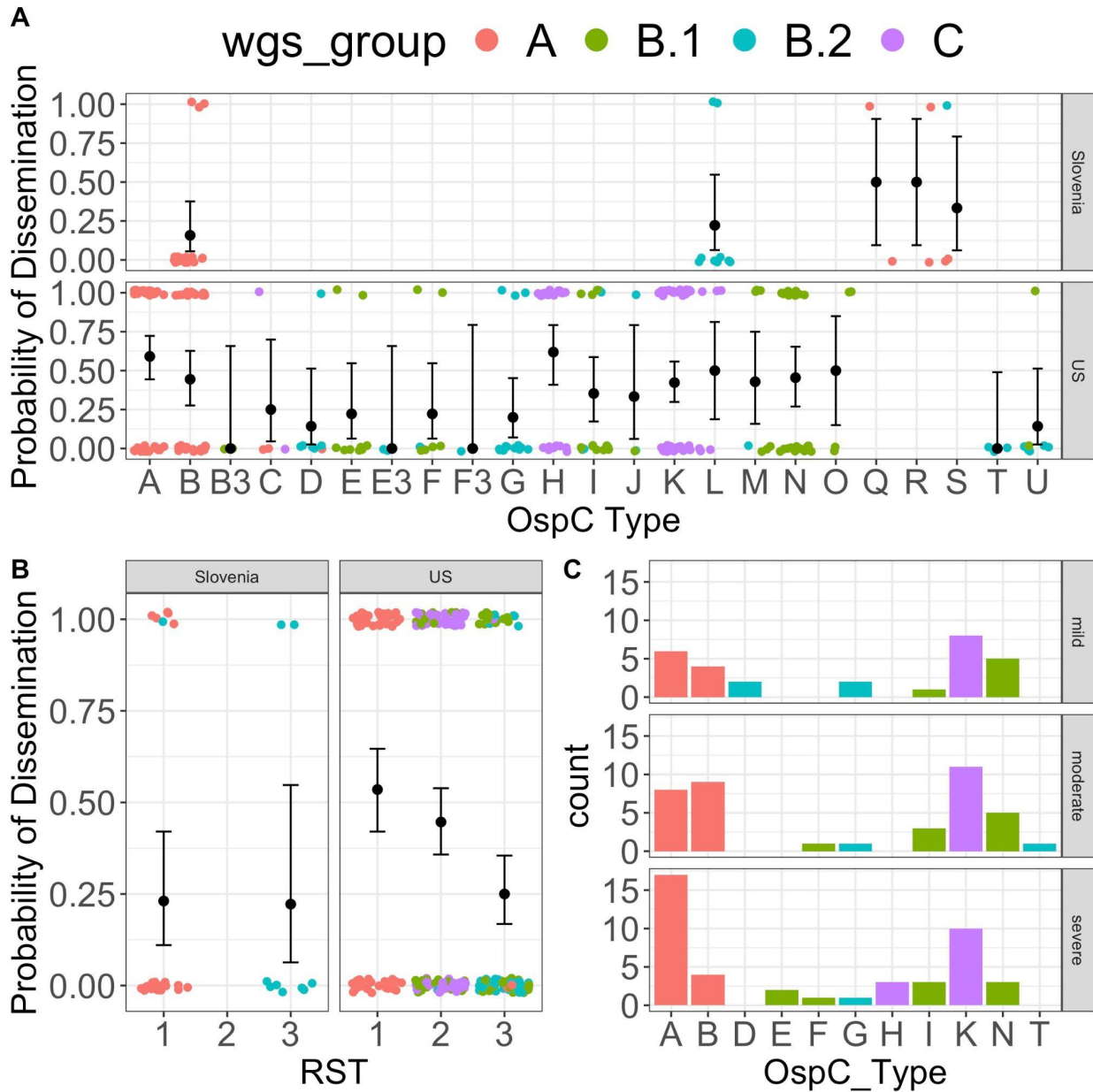
767
768



769
770
771
772
773
774
775
776
777

Supplemental Figure 3: **A.** Core genome phylogenetic tree colored by WGS groups A-C with group B divided into B.1 and B.2; accessory genome presence/absence matrix is reproduced from Figure 5 to highlight accessory genome elements that correlate with B.1 and B.2 sublineages. The clade corresponding to RST1 is shaded in light blue and the clade corresponding to OspC type A is shaded in green. **B.** MDS plot with group B divided into B.1 and B.2. **C.** Probability of dissemination by genomic group using the four groups including B.1 and B.2.

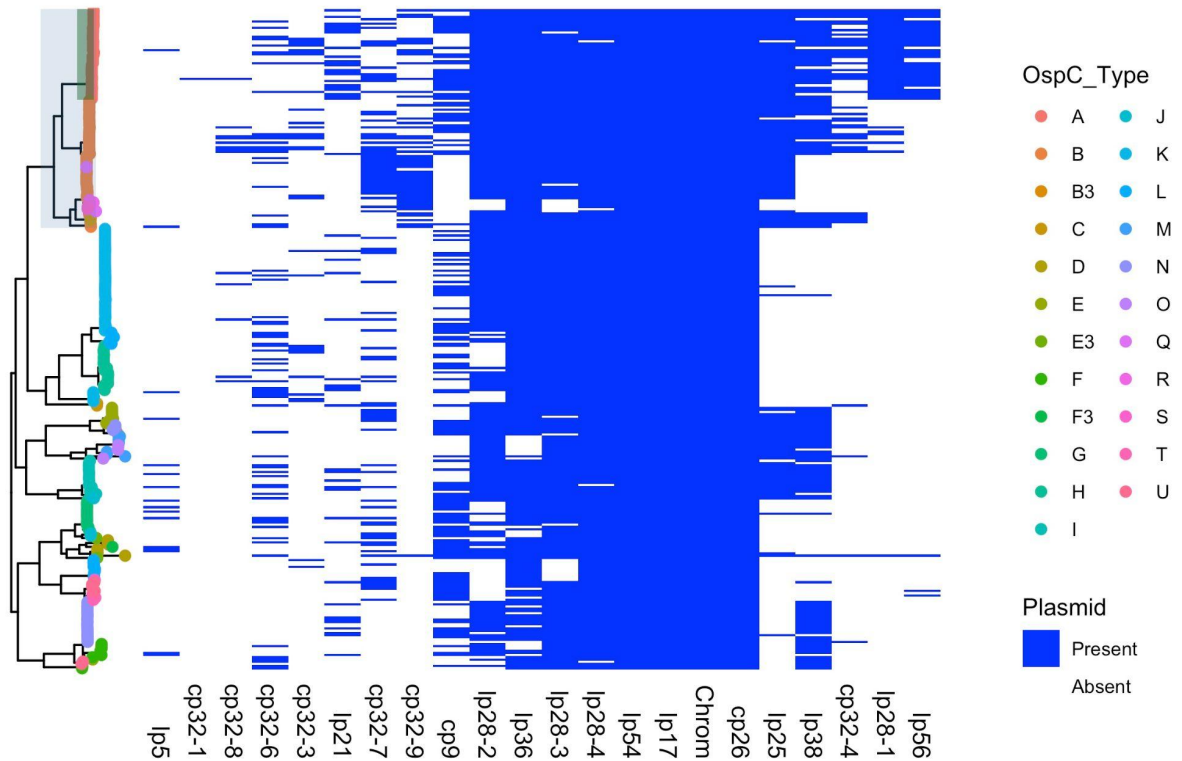
778
779



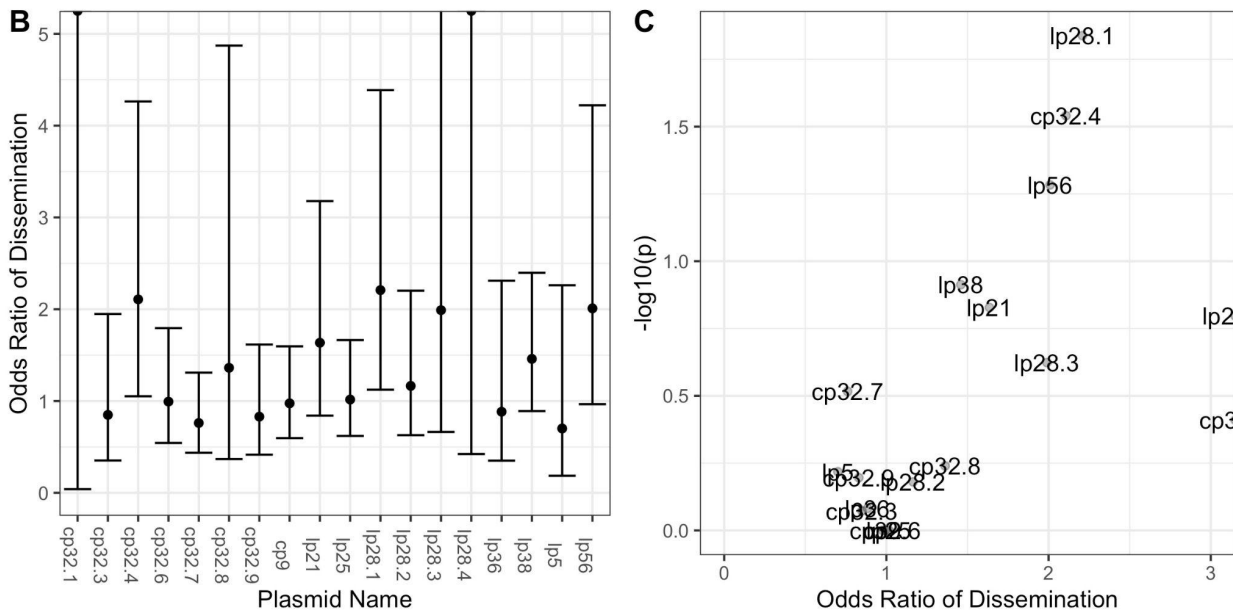
780
781
782
783

Supplemental Figure 4: Probability of dissemination by **(A)** OspC type and **(B)** RST. **C.** Severity of Lyme disease by OspC type with WGS group shown by color.

784 **A**



785



786

787

788

789

790

791

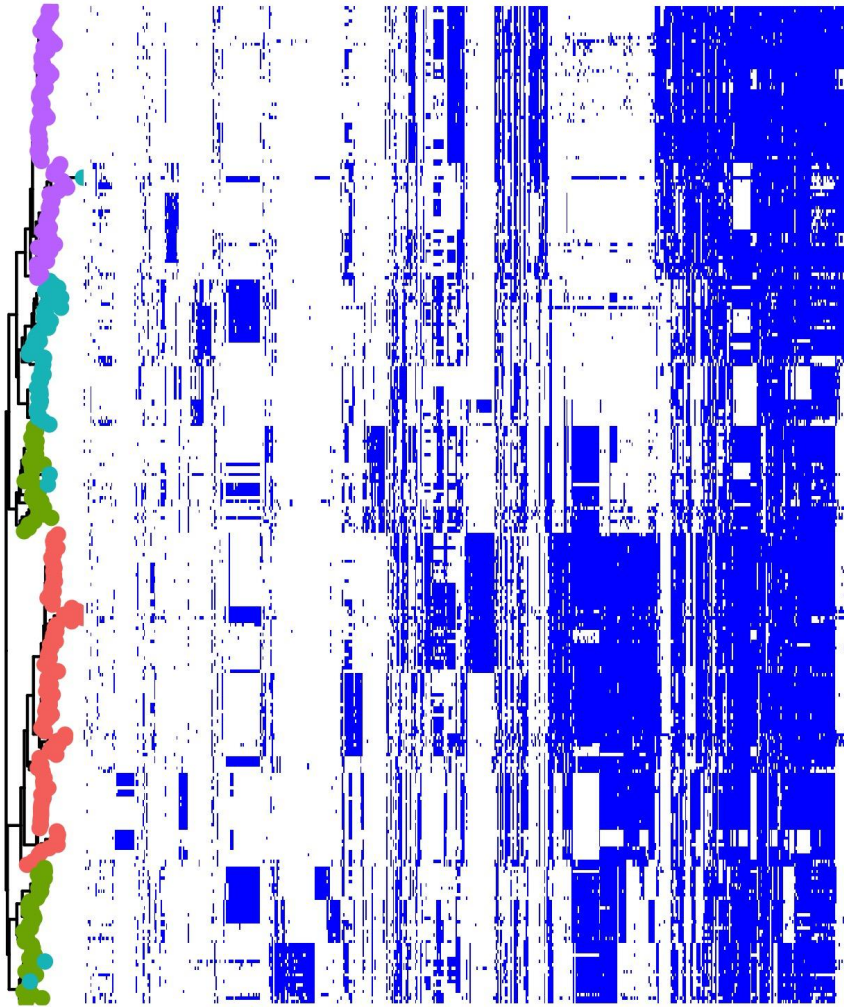
792

793

Supplemental Figure 5: A. Inferred presence / absence of a plasmid based on alignment of assembly contigs to the B31 reference. A plasmid is inferred as ‘present’ in the isolate if > 50% of the length is covered by aligned contigs in the de novo assembly for the genome of the corresponding isolate. The clade corresponding to RST1 is shaded in light blue and the clade corresponding to OspC type A is shaded in green. **B.** Odds ratio of dissemination and confidence interval by plasmid, inferred by Pfam32 sequences. **C.** Volcano plot displaying the -

794 log₁₀ P value (as calculated using Fisher's exact test) and the odds ratio of dissemination for
795 each plasmid, inferred by alignment of assembled contigs to the B31 reference sequence.

796 A



wgs_group

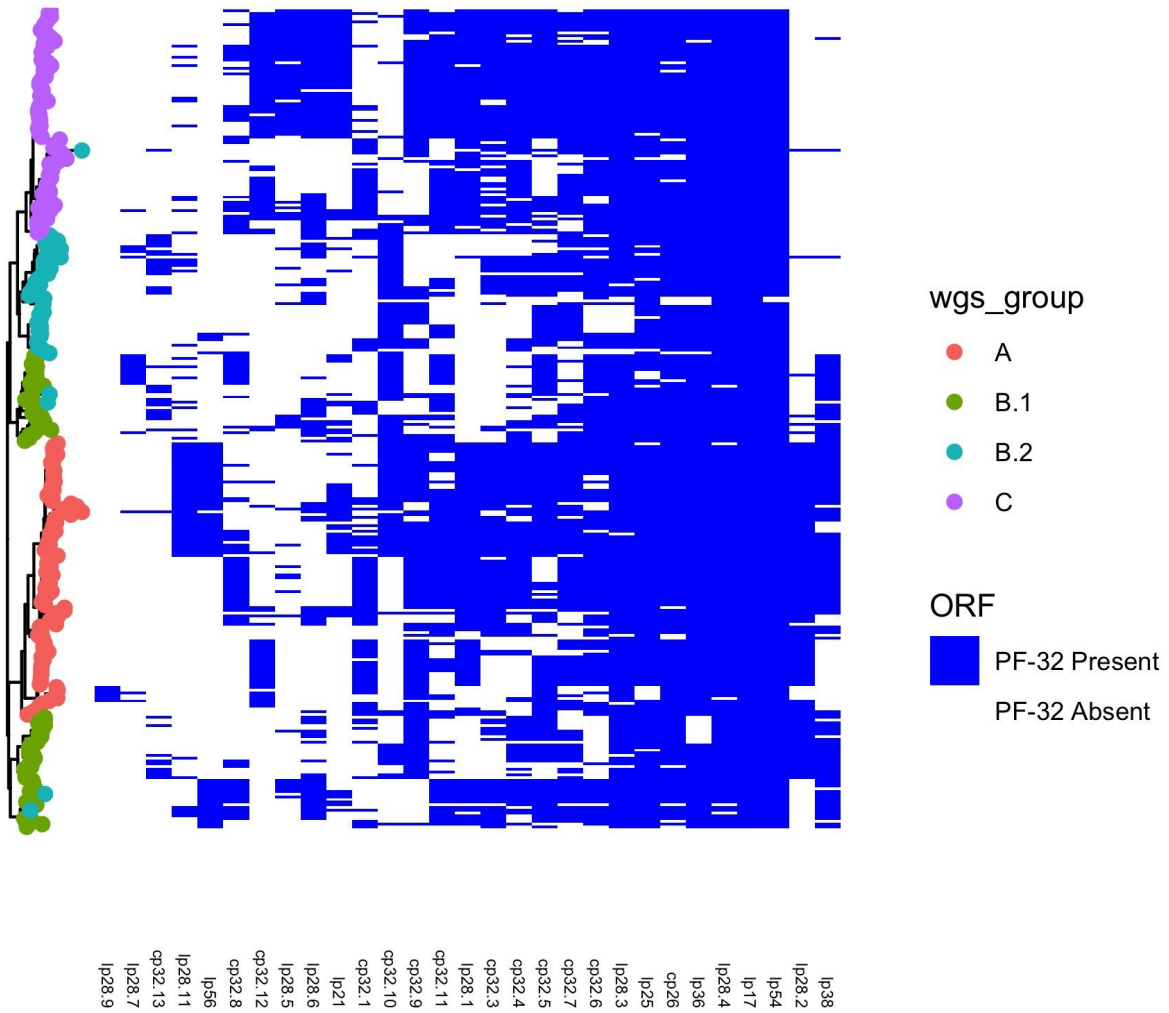
- A
- B.1
- B.2
- C

Class

- ORF Present
- ORF Absent

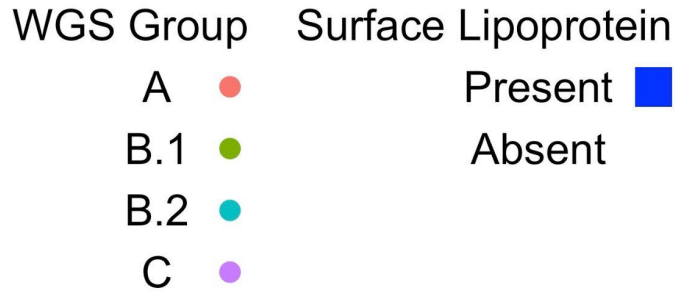
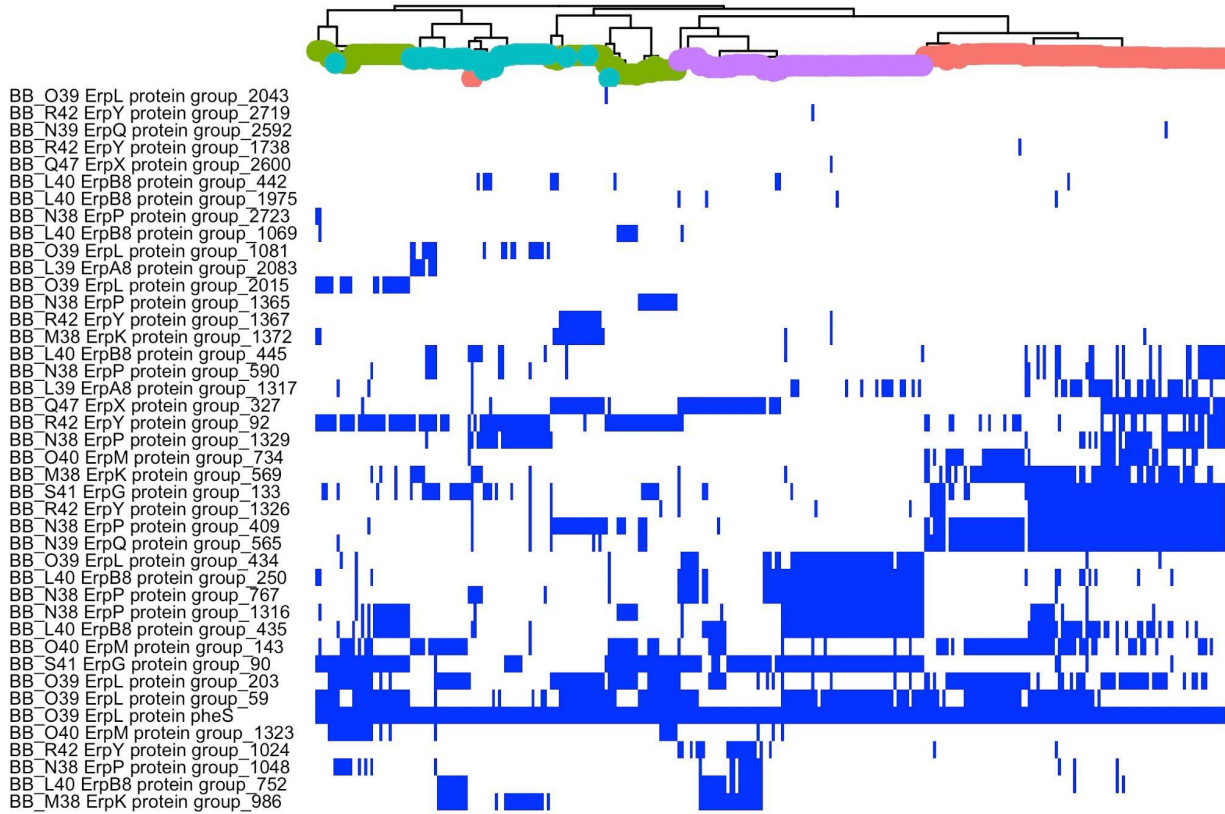
797
798

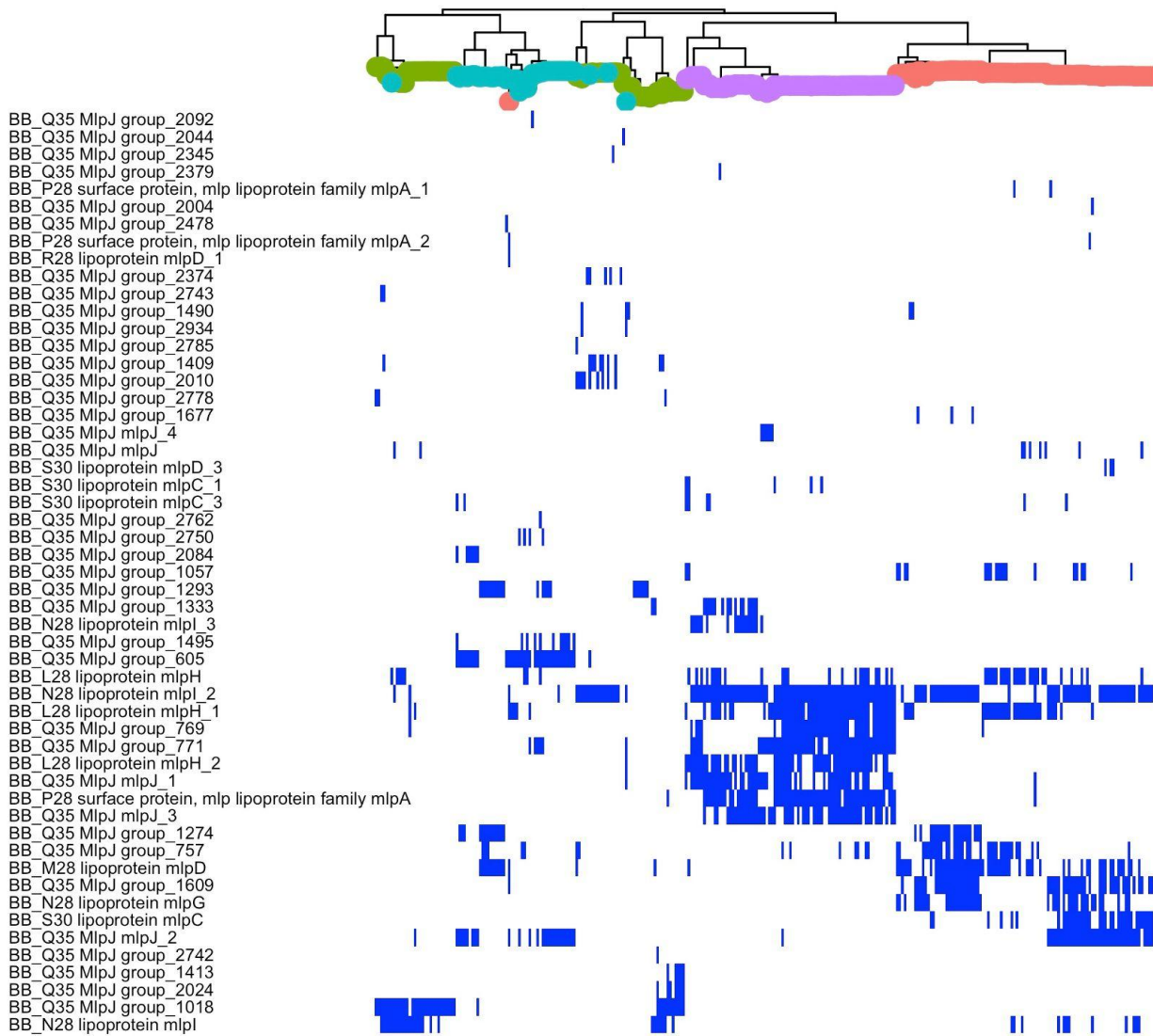
799 B



800
801
802
803
804
805

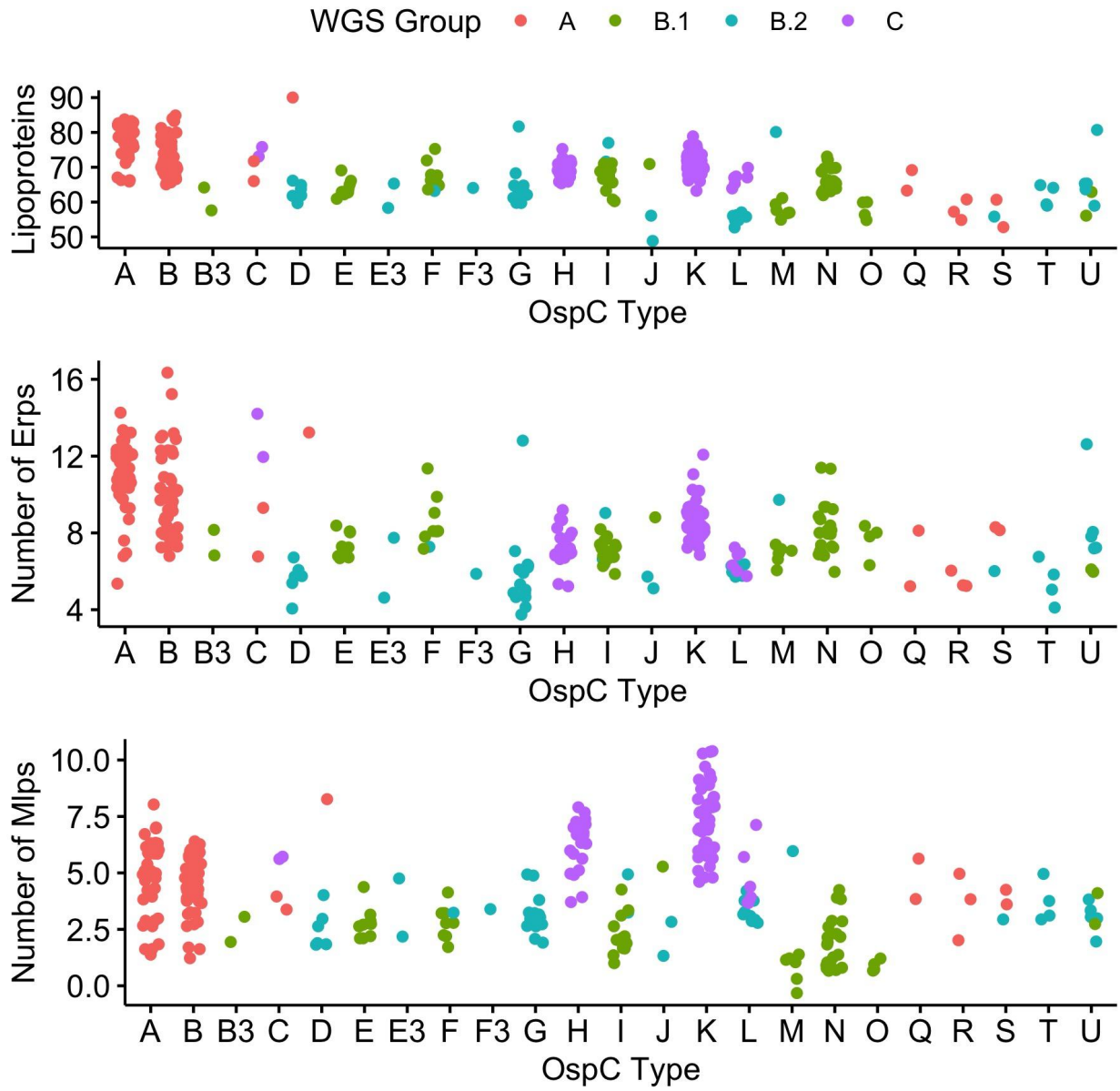
Supplemental Figure 6: A. Phylogenetic tree created from the accessory genome with accessory genome elements plotted according to their presence/absence in individual strains. **B.** Phylogenetic tree created from the accessory genome with PFam32 plasmid compatibility sequences plotted according to the presence/absence in individual strains.





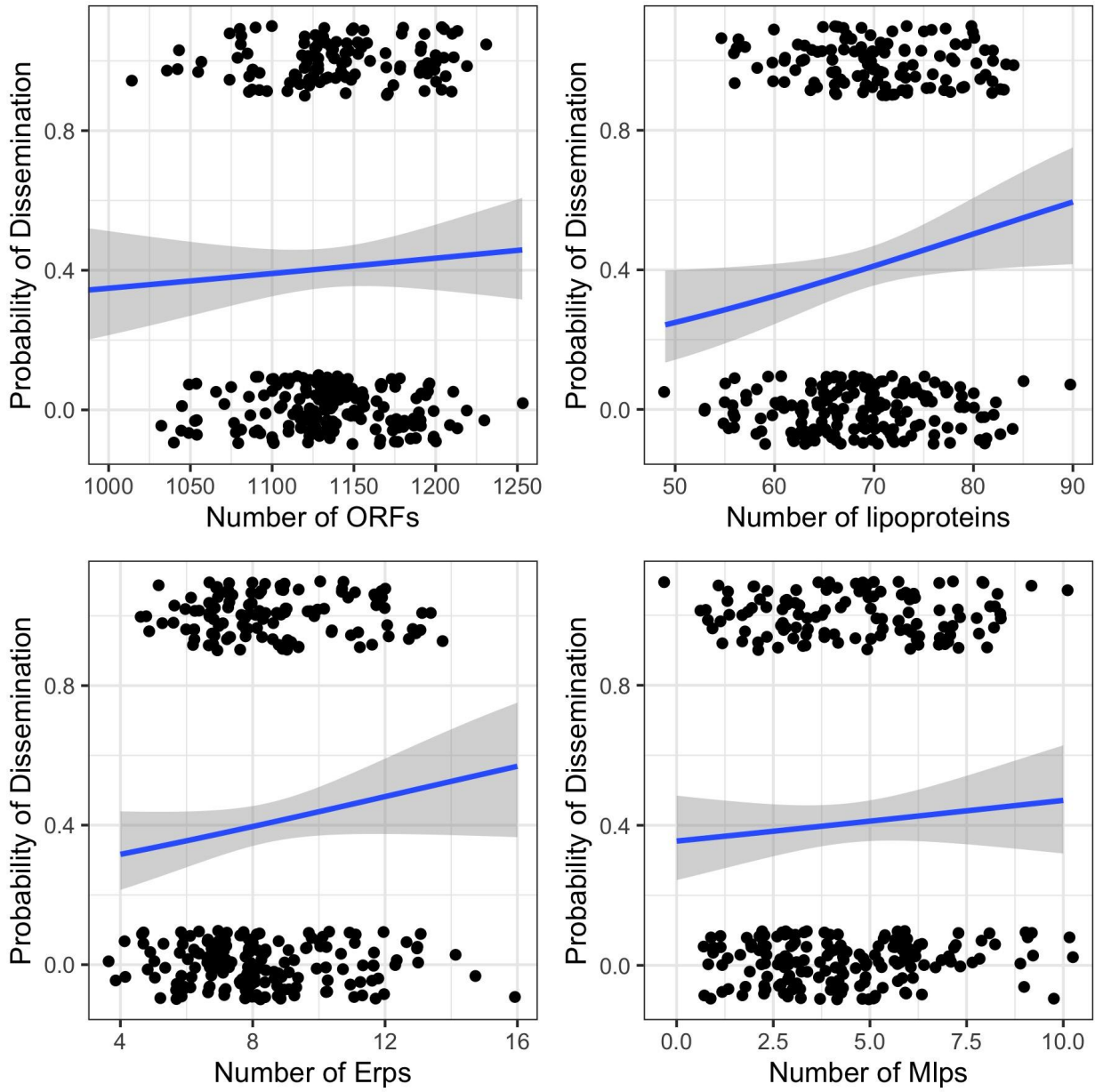
WGS Group	Surface Lipoprotein
A ●	Present ■
B.1 ●	Absent
B.2 ●	
C ●	

811 C



812
813

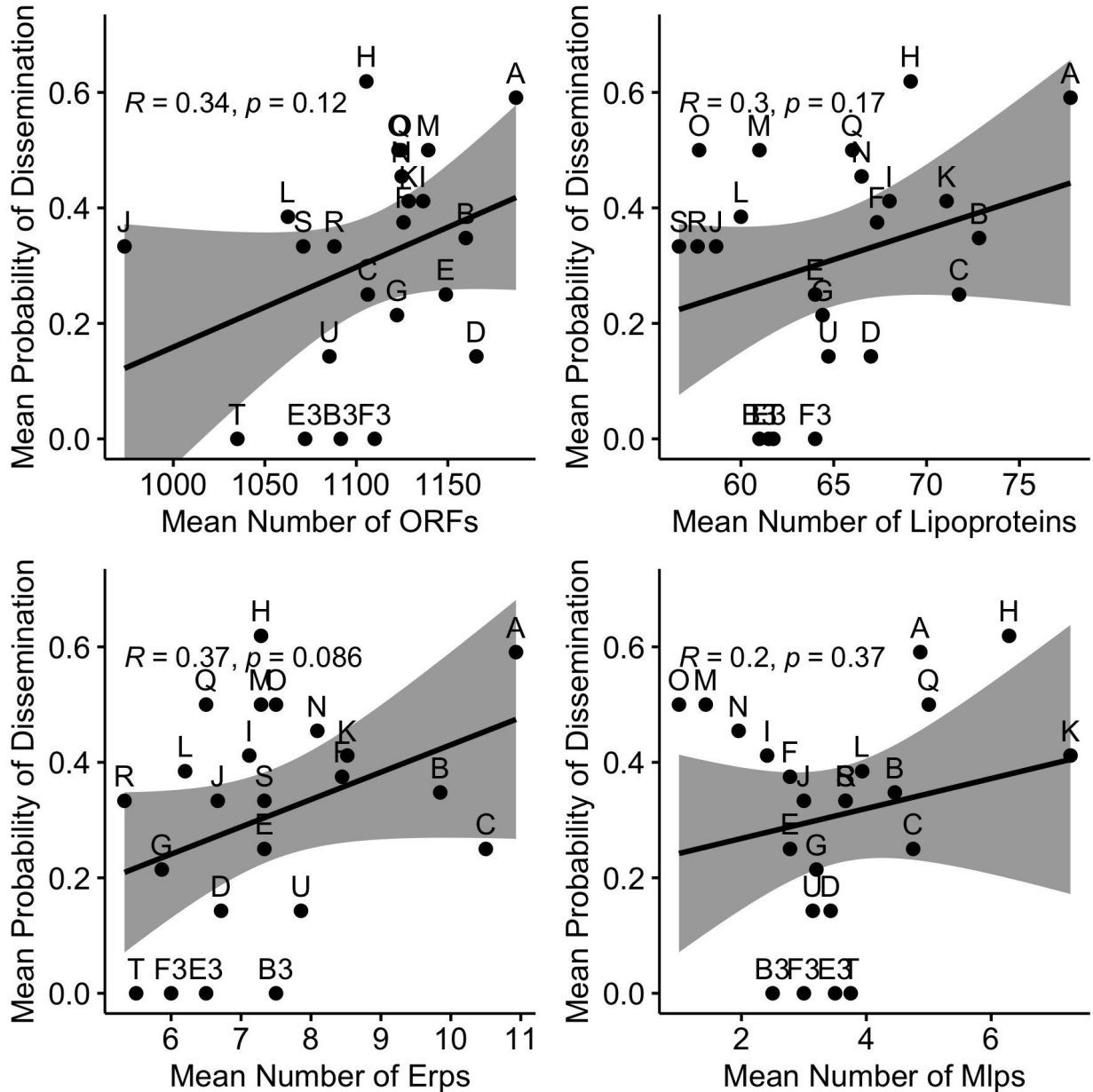
814 **D**



815
816

817
818

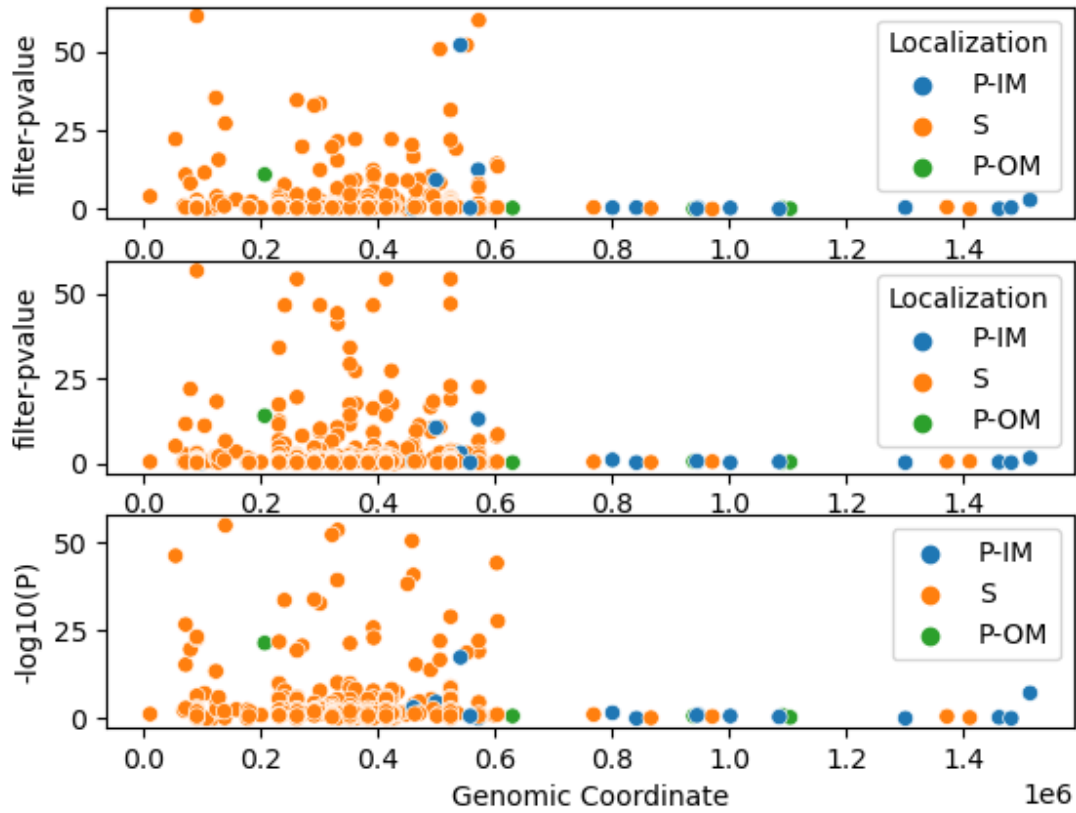
E



819
820
821
822
823
824
825
826
827
828
829
830

Supplemental Figure 7: A and B. Core genome phylogeny with presence/absence of Erp (C) orthologs and Mlp (D) orthologs. **C.** The number of surface-exposed lipoproteins (top panel), Erps (middle panel), and Mlps (bottom panel) by OspC type. **D.** Probability of dissemination by number of ORF (top left, logistic regression coefficient for slope, $\beta_1 = 0.002 \pm 0.002$, $p = 0.450$), number of surface-exposed lipoproteins (top right, $\beta_1 = 0.037 \pm 0.017$, $p = 0.03$, logistic regression), number of Erps (bottom left, $\beta_1 = 0.087 \pm 0.053$, $p = 0.10$, logistic regression), and number of Mlps (bottom right, $\beta_1 = 0.048 \pm 0.055$, $p = 0.38$, logistic regression). **E.** For each OspC type, mean probability of dissemination vs mean number of ORF (top left), mean number of surface-exposed lipoproteins (top right), mean number of Erps (bottom left), and mean number of Mlps (bottom right).

831



832

833 **Supplemental Figure 8:** Manhattan Plots showing the association of individual lipoproteins with
834 OspC type A (top panel), Osp C type K (middle panel), and RST1 (bottom panel). Individual
835 lipoproteins are annotated by their localization. P-IM: Periplasmic inner membrane. P-OM:
836 Periplasmic outer membrane. S: surface.

837

838

839 **List of supplemental data files**

- 840 Supplemental Table 1: Summary table of isolates and phenotypes
- 841 Supplemental Table 2: List of isolates and phenotypes
- 842 Supplemental Table 3: Assembly statistics
- 843 Supplemental Table 4: Association statistics for plasmids, as inferred from PFam32 types.
- 844 Supplemental Table 5: Association statistics for plasmids, as inferred from B31 reference
- 845 Supplemental Table 5: Association statistics for lineage model
- 846 Supplemental Table 6: Association statistics for lineage model restricted to surface lipoproteins
- 847 Supplemental Table 7: Association statistics for OspC type A associations
- 848 Supplemental Table 8: Association statistics for OspC type K associations
- 849 Supplemental Table 9: Association statistics for RST1 associations
- 850 Supplemental Data File 1: List of ortholog groups with reference sequences
- 851 Supplemental Data File 2: High resolution version of presence/absence matrix in Figure 5B.
- 852

853

854 **Supplemental Note 1:**

855 The clock rate (in substitutions/site/year) for our initial model using a non-informative (CTMC
856 rate reference) prior failed to converge—resulting in posterior 95% posterior density range from
857 5×10^{-25} substitutions/site/year to 1.2×10^{-8} substitutions/site/year—the implausibly small values
858 at the lower end of the range are indicative of an insufficient temporal signal associated with
859 genetic diversity in the core genome to establish an estimate without a priori assumptions.
860 However, the inferred clock rate posterior had a clear single mode and a reasonable posterior
861 mean (1.8×10^{-9} substitutions/site/year). To address this, we incorporated a priori information on
862 mutation (gamma prior with shape 2, scale 1×10^{-9} , for which 95% of the density is between 3.55
863 $\times 10^{-10}$ substitutions/site/year and 4.47×10^{-9} substitutions/site/year, concordant with previous
864 suggestions that the rate is approximately 1×10^{-9} substitutions/site/year[52]). This analysis
865 suggests that the common ancestry of circulating human-infectious populations was remote
866 (95% posterior density for Midwest strains: 380,000 - 11.8 million years; 95% posterior density
867 for Slovenian strains: 379,000 - 11.5 million years; all strains: 380,000 years, 11.8 million years)
868 (Figure 2E-F). We also ran models with a fixed rate across a variety of reasonable values ($1e-$
869 10 to $1e-8$) (Figure 2G).

870 **References**

- 871 1. Radolf JD, Strle K, Lemieux JE, Strle F. Lyme Disease in Humans. *Curr Issues Mol Biol.*
872 2021;42: 333–384.
- 873 2. Lantos PM, Rumbaugh J, Bockenstedt LK, Falck-Ytter YT, Aguero-Rosenfeld ME,
874 Auwaerter PG, et al. Clinical practice guidelines by the Infectious Diseases Society of
875 America (IDSA), American Academy of Neurology (AAN), and American College of
876 Rheumatology (ACR): 2020 guidelines for the prevention, diagnosis and treatment of Lyme
877 disease. *Clin Infect Dis.* 2021;72: e1–e48.
- 878 3. Strle K, Jones KL, Drouin EE, Li X, Steere AC. *Borrelia burgdorferi* RST1 (OspC type A)
879 genotype is associated with greater inflammation and more severe Lyme disease. *Am J*
880 *Pathol.* 2011;178: 2726–2739.
- 881 4. Wormser GP, Brisson D, Liveris D, Hanincová K, Sandigursky S, Nowakowski J, et al.
882 *Borrelia burgdorferi* genotype predicts the capacity for hematogenous dissemination during
883 early Lyme disease. *J Infect Dis.* 2008;198: 1358–1364.
- 884 5. Wormser GP, Liveris D, Nowakowski J, Nadelman RB, Cavaliere LF, McKenna D, et al.
885 Association of specific subtypes of *Borrelia burgdorferi* with hematogenous dissemination in
886 early Lyme disease. *J Infect Dis.* 1999;180: 720–725.
- 887 6. Wang G, Ojaimi C, Wu H, Saksenberg V, Iyer R, Liveris D, et al. Disease severity in a
888 murine model of Lyme borreliosis is associated with the genotype of the infecting *Borrelia*
889 *burgdorferi sensu stricto* strain. *J Infect Dis.* 2002;186: 782–791.
- 890 7. Wang G, van Dam AP, Schwartz I, Dankert J. Molecular typing of *Borrelia burgdorferi*
891 *sensu lato*: taxonomic, epidemiological, and clinical implications. *Clin Microbiol Rev.*
892 1999;12: 633–653.
- 893 8. Wang G, Ojaimi C, Iyer R, Saksenberg V, McClain SA, Wormser GP, et al. Impact of
894 genotypic variation of *Borrelia burgdorferi sensu stricto* on kinetics of dissemination and
895 severity of disease in C3H/HeJ mice. *Infect Immun.* 2001;69: 4303–4312.
- 896 9. Fraser CM, Casjens S, Huang WM, Sutton GG, Clayton R, Lathigra R, et al. Genomic
897 sequence of a Lyme disease spirochaete, *Borrelia burgdorferi*. *Nature.* 1997;390: 580–586.
- 898 10. Casjens S, Palmer N, van Vugt R, Huang WM, Stevenson B, Rosa P, et al. A bacterial
899 genome in flux: the twelve linear and nine circular extrachromosomal DNAs in an infectious
900 isolate of the Lyme disease spirochete *Borrelia burgdorferi*. *Mol Microbiol.* 2000;35: 490–
901 516.
- 902 11. Casjens S, van Vugt R, Tilly K, Rosa PA, Stevenson B. Homology throughout the multiple
903 32-kilobase circular plasmids present in Lyme disease spirochetes. *J Bacteriol.* 1997;179:
904 217–227.
- 905 12. Casjens SR, Di L, Akther S, Mongodin EF, Luft BJ, Schutzer SE, et al. Primordial origin and
906 diversification of plasmids in Lyme disease agent bacteria. *BMC Genomics.* 2018;19: 218.
- 907 13. Margos G, Hepner S, Mang C, Marosevic D, Reynolds SE, Krebs S, et al. Lost in plasmids:

- 908 next generation sequencing and the complex genome of the tick-borne pathogen *Borrelia*
909 *burgdorferi*. *BMC Genomics*. 2017;18: 422.
- 910 14. Tyler S, Tyson S, Dibernardo A, Drebot M, Feil EJ, Graham M, et al. Whole genome
911 sequencing and phylogenetic analysis of strains of the agent of Lyme disease *Borrelia*
912 *burgdorferi* from Canadian emergence zones. *Sci Rep*. 2018;8: 10552.
- 913 15. Castillo-Ramírez S, Fingerle V, Jungnick S, Straubinger RK, Krebs S, Blum H, et al. Trans-
914 Atlantic exchanges have shaped the population structure of the Lyme disease agent
915 *Borrelia burgdorferi sensu stricto*. *Sci Rep*. 2016;6: 22794.
- 916 16. Walter KS, Carpi G, Caccone A, Diuk-Wasser MA. Genomic insights into the ancient
917 spread of Lyme disease across North America. *Nat Ecol Evol*. 2017;1: 1569–1576.
- 918 17. Di L, Pagan PE, Packer D, Martin CL, Akther S, Ramrattan G, et al. *BorreliaBase*: a
919 phylogeny-centered browser of *Borrelia* genomes. *BMC Bioinformatics*. 2014;15: 233.
- 920 18. Carpi G, Walter KS, Bent SJ, Hoen AG, Diuk-Wasser M, Caccone A. Whole genome
921 capture of vector-borne pathogens from mixed DNA samples: a case study of *Borrelia*
922 *burgdorferi*. *BMC Genomics*. 2015;16: 434.
- 923 19. Schutzer SE, Fraser-Liggett CM, Casjens SR, Qiu W-G, Dunn JJ, Mongodin EF, et al.
924 Whole-genome sequences of thirteen isolates of *Borrelia burgdorferi*. *J Bacteriol*. 2011;193:
925 1018–1020.
- 926 20. Wang G, Liveris D, Mukherjee P, Jungnick S, Margos G, Schwartz I. Molecular Typing of
927 *Borrelia burgdorferi*. *Curr Protoc Microbiol*. 2014;34: 12C.5.1–31.
- 928 21. Liveris D, Gazumyan A, Schwartz I. Molecular typing of *Borrelia burgdorferi sensu lato* by
929 PCR-restriction fragment length polymorphism analysis. *J Clin Microbiol*. 1995;33: 589–
930 595.
- 931 22. Liveris D, Wormser GP, Nowakowski J, Nadelman R, Bittker S, Cooper D, et al. Molecular
932 typing of *Borrelia burgdorferi* from Lyme disease patients by PCR-restriction fragment
933 length polymorphism analysis. *J Clin Microbiol*. 1996;34: 1306–1309.
- 934 23. Qiu W-G, Schutzer SE, Bruno JF, Attie O, Xu Y, Dunn JJ, et al. Genetic exchange and
935 plasmid transfers in *Borrelia burgdorferi sensu stricto* revealed by three-way genome
936 comparisons and multilocus sequence typing. *Proc Natl Acad Sci U S A*. 2004;101: 14150–
937 14155.
- 938 24. Bunikis J, Garpmo U, Tsao J, Berglund J, Fish D, Barbour AG. Sequence typing reveals
939 extensive strain diversity of the Lyme borreliosis agents *Borrelia burgdorferi* in North
940 America and *Borrelia afzelii* in Europe. *Microbiology*. 2004;150: 1741–1755.
- 941 25. Barbour AG, Travinsky B. Evolution and distribution of the *ospC* Gene, a transferable
942 serotype determinant of *Borrelia burgdorferi*. *MBio*. 2010;1. Available:
943 <https://www.ncbi.nlm.nih.gov/pubmed/20877579>
- 944 26. Cerar T, Strle F, Stupica D, Ruzic-Sabljić E, McHugh G, Steere AC, et al. Differences in
945 Genotype, Clinical Features, and Inflammatory Potential of *Borrelia burgdorferi sensu*
946 *stricto* Strains from Europe and the United States. *Emerg Infect Dis*. 2016;22: 818–827.

- 947 27. Hanincova K, Mukherjee P, Ogden NH, Margos G, Wormser GP, Reed KD, et al. Multilocus
948 sequence typing of *Borrelia burgdorferi* suggests existence of lineages with differential
949 pathogenic properties in humans. *PLoS One*. 2013;8: e73066.
- 950 28. Margos G, Gatewood AG, Aanensen DM, Hanincová K, Terekhova D, Vollmer SA, et al.
951 MLST of housekeeping genes captures geographic population structure and suggests a
952 European origin of *Borrelia burgdorferi*. *Proc Natl Acad Sci U S A*. 2008;105: 8730–8735.
- 953 29. Strle K, Shin JJ, Glickstein LJ, Steere AC. Association of a Toll-like receptor 1
954 polymorphism with heightened Th1 inflammatory responses and antibiotic-refractory Lyme
955 arthritis. *Arthritis Rheum*. 2012;64: 1497–1507.
- 956 30. Jones KL, Glickstein LJ, Damle N, Sikand VK, McHugh G, Steere AC. *Borrelia burgdorferi*
957 genetic markers and disseminated disease in patients with early Lyme disease. *J Clin*
958 *Microbiol*. 2006;44: 4407–4413.
- 959 31. Dykhuizen DE, Brisson D, Sandigursky S, Wormser GP, Nowakowski J, Nadelman RB, et
960 al. The Propensity of Different *Borrelia burgdorferi sensu stricto* Genotypes to Cause
961 Disseminated Infections in Humans. *Am J Trop Med Hyg*. 2008;78: 806–810.
- 962 32. Brisson D, Baxamusa N, Schwartz I, Wormser GP. Biodiversity of *Borrelia burgdorferi*
963 strains in tissues of Lyme disease patients. *PLoS One*. 2011;6: e22926.
- 964 33. Ružić-Sabljić E, Maraspin V, Stupica D, Rojko T, Bogovič P, Strle F, et al. Comparison of
965 MKP and BSK-H media for the cultivation and isolation of *Borrelia burgdorferi sensu lato*.
966 *PLoS One*. 2017;12: e0171622.
- 967 34. Wang G, Iyer R, Bittker S, Cooper D, Small J, Wormser GP, et al. Variations in Barbour-
968 Stoenner-Kelly culture medium modulate infectivity and pathogenicity of *Borrelia burgdorferi*
969 clinical isolates. *Infect Immun*. 2004;72: 6702–6706.
- 970 35. Centers for Disease Control and Prevention (CDC). Recommendations for test
971 performance and interpretation from the Second National Conference on Serologic
972 Diagnosis of Lyme Disease. *MMWR Morb Mortal Wkly Rep*. 1995;44: 590–591.
- 973 36. Mygland A, Ljøstad U, Fingerle V, Rupprecht T, Schmutzhard E, Steiner I, et al. EFNS
974 guidelines on the diagnosis and management of European Lyme neuroborreliosis. *Eur J*
975 *Neurol*. 2010;17: 8–16, e1–4.
- 976 37. Bolger AM, Lohse M, Usadel B. Trimmomatic: a flexible trimmer for Illumina sequence data.
977 *Bioinformatics*. 2014;30: 2114–2120.
- 978 38. Bankevich A, Nurk S, Antipov D, Gurevich AA, Dvorkin M, Kulikov AS, et al. SPAdes: a new
979 genome assembly algorithm and its applications to single-cell sequencing. *J Comput Biol*.
980 2012;19: 455–477.
- 981 39. Gurevich A, Saveliev V, Vyahhi N, Tesler G. QUAST: quality assessment tool for genome
982 assemblies. *Bioinformatics*. 2013;29: 1072–1075.
- 983 40. Wood DE, Lu J, Langmead B. Improved metagenomic analysis with Kraken 2. *Genome*
984 *Biol*. 2019;20: 257.
- 985 41. Jolley KA, Maiden MCJ. BIGSdb: Scalable analysis of bacterial genome variation at the

- 986 population level. BMC Bioinformatics. 2010;11: 595.
- 987 42. Murray KD, Webers C, Ong CS, Borevitz J, Warthmann N. kWIP: The k-mer weighted inner
988 product, a de novo estimator of genetic similarity. PLoS Comput Biol. 2017;13: e1005727.
- 989 43. Seemann T. Prokka: rapid prokaryotic genome annotation. Bioinformatics. 2014;30: 2068–
990 2069.
- 991 44. Page AJ, Cummins CA, Hunt M, Wong VK, Reuter S, Holden MTG, et al. Roary: rapid
992 large-scale prokaryote pan genome analysis. Bioinformatics. 2015;31: 3691–3693.
- 993 45. Price MN, Dehal PS, Arkin AP. FastTree 2--approximately maximum-likelihood trees for
994 large alignments. PLoS One. 2010;5: e9490.
- 995 46. Gentleman RC, Carey VJ, Bates DM, Bolstad B, Dettling M, Dudoit S, et al. Bioconductor:
996 open software development for computational biology and bioinformatics. Genome Biol.
997 2004;5: R80.
- 998 47. Ihaka R, Gentleman R. R: A Language for Data Analysis and Graphics. J Comput Graph
999 Stat. 1996;5: 299–314.
- 1000 48. Wickham H, Others. Tidyverse: Easily install and load the “tidyverse.” R package version.
1001 2017;1: 2017.
- 1002 49. Yu G, Smith DK, Zhu H, Guan Y, Lam TT. ggtree : an r package for visualization and
1003 annotation of phylogenetic trees with their covariates and other associated data. McInerney
1004 G, editor. Methods Ecol Evol. 2017;8: 28–36.
- 1005 50. Eddy SR. A new generation of homology search tools based on probabilistic inference.
1006 Genome Inform. 2009;23: 205–211.
- 1007 51. Schwartz I, Margos G, Casjens SR, Qiu W-G, Eggers CH. Multipartite Genome of Lyme
1008 Disease *Borrelia*: Structure, Variation and Prophages. Curr Issues Mol Biol. 2021;42: 409–
1009 454.
- 1010 52. Hoen AG, Margos G, Bent SJ, Diuk-Wasser MA, Barbour A, Kurtenbach K, et al.
1011 Phylogeography of *Borrelia burgdorferi* in the eastern United States reflects multiple
1012 independent Lyme disease emergence events. Proc Natl Acad Sci U S A. 2009;106:
1013 15013–15018.
- 1014 53. Radolf JD, Caimano MJ, Stevenson B, Hu LT. Of ticks, mice and men: understanding the
1015 dual-host lifestyle of Lyme disease spirochaetes. Nat Rev Microbiol. 2012;10: 87–99.
- 1016 54. Brisson D, Drecktrah D, Eggers CH, Samuels DS. Genetics of *Borrelia burgdorferi*. Annu
1017 Rev Genet. 2012;46: 515–536.
- 1018 55. Steere AC, Strle F, Wormser GP, Hu LT, Branda JA, Hovius JWR, et al. Lyme borreliosis.
1019 Nat Rev Dis Primers. 2016;2: 16090.
- 1020 56. Dowdell AS, Murphy MD, Azodi C, Swanson SK, Florens L, Chen S, et al. Comprehensive
1021 Spatial Analysis of the *Borrelia burgdorferi* Lipoproteome Reveals a Compartmentalization
1022 Bias toward the Bacterial Surface. J Bacteriol. 2017;199. doi:10.1128/JB.00658-16

- 1023 57. Stevenson B, Tilly K, Rosa PA. A family of genes located on four separate 32-kilobase
1024 circular plasmids in *Borrelia burgdorferi* B31. *J Bacteriol.* 1996;178: 3508–3516.
- 1025 58. Brissette CA, Cooley AE, Burns LH, Riley SP, Verma A, Woodman ME, et al. Lyme
1026 borreliosis spirochete Erp proteins, their known host ligands, and potential roles in
1027 mammalian infection. *Int J Med Microbiol.* 2008;298: 257–267.
- 1028 59. Porcella SF, Popova TG, Akins DR, Li M, Radolf JD, Norgard MV. *Borrelia burgdorferi*
1029 supercoiled plasmids encode multicopy tandem open reading frames and a lipoprotein
1030 gene family. *J Bacteriol.* 1996;178: 3293–3307.
- 1031 60. Porcella SF, Fitzpatrick CA, Bono JL. Expression and Immunological Analysis of the
1032 Plasmid-Borne mlp Genes of *Borrelia burgdorferi* Strain B31. *Infect Immun.* 2000;68: 4992–
1033 5001.
- 1034 61. Earle SG, Wu C-H, Charlesworth J, Stoesser N, Gordon NC, Walker TM, et al. Identifying
1035 lineage effects when controlling for population structure improves power in bacterial
1036 association studies. *Nat Microbiol.* 2016;1: 16041.
- 1037 62. Lees JA, Vehkala M, Välimäki N, Harris SR, Chewapreecha C, Croucher NJ, et al.
1038 Sequence element enrichment analysis to determine the genetic basis of bacterial
1039 phenotypes. *Nat Commun.* 2016;7: 12797.
- 1040 63. Terekhova D, Iyer R, Wormser GP, Schwartz I. Comparative genome hybridization reveals
1041 substantial variation among clinical isolates of *Borrelia burgdorferi sensu stricto* with
1042 different pathogenic properties. *J Bacteriol.* 2006;188: 6124–6134.
- 1043 64. Qiu W-G, Bruno JF, McCaig WD, Xu Y, Livey I, Schriefer ME, et al. Wide distribution of a
1044 high-virulence *Borrelia burgdorferi* clone in Europe and North America. *Emerg Infect Dis.*
1045 2008;14: 1097–1104.
- 1046 65. Mongodin EF, Casjens SR, Bruno JF, Xu Y, Drabek EF, Riley DR, et al. Inter- and intra-
1047 specific pan-genomes of *Borrelia burgdorferi sensu lato*: genome stability and adaptive
1048 radiation. *BMC Genomics.* 2013;14: 693.
- 1049 66. Labandeira-Rey M, Skare JT. Decreased infectivity in *Borrelia burgdorferi* strain B31 is
1050 associated with loss of linear plasmid 25 or 28-1. *Infect Immun.* 2001;69: 446–455.
- 1051 67. Magunda PRH, Bankhead T. Investigating the potential role of non-vls genes on linear
1052 plasmid 28–1 in virulence and persistence by *Borrelia burgdorferi*. *BMC Microbiol.* 2016;16:
1053 180.
- 1054 68. Labandeira-Rey M, Seshu J, Skare JT. The absence of linear plasmid 25 or 28-1 of *Borrelia*
1055 *burgdorferi* dramatically alters the kinetics of experimental infection via distinct
1056 mechanisms. *Infect Immun.* 2003;71: 4608–4613.
- 1057 69. Purser JE, Norris SJ. Correlation between plasmid content and infectivity in *Borrelia*
1058 *burgdorferi*. *Proc Natl Acad Sci U S A.* 2000;97: 13865–13870.
- 1059 70. Lawrenz MB, Kawabata H, Purser JE, Norris SJ. Decreased electroporation efficiency in
1060 *Borrelia burgdorferi* containing linear plasmids lp25 and lp56: impact on transformation of
1061 infectious *B. burgdorferi*. *Infect Immun.* 2002;70: 4798–4804.

- 1062 71. Rego ROM, Bestor A, Rosa PA. Defining the plasmid-borne restriction-modification
1063 systems of the Lyme disease spirochete *Borrelia burgdorferi*. *J Bacteriol.* 2011;193: 1161–
1064 1171.
- 1065 72. Lin Y-P, Benoit V, Yang X, Martínez-Herranz R, Pal U, Leong JM. Strain-specific variation
1066 of the decorin-binding adhesin DbpA influences the tissue tropism of the Lyme disease
1067 spirochete. *PLoS Pathog.* 2014;10: e1004238.
- 1068 73. Lin Y-P, Tan X, Caine JA, Castellanos M, Chaconas G, Coburn J, et al. Strain-specific joint
1069 invasion and colonization by Lyme disease spirochetes is promoted by outer surface
1070 protein C. *PLoS Pathog.* 2020;16: e1008516.
- 1071 74. Caine JA, Lin Y-P, Kessler JR, Sato H, Leong JM, Coburn J. *Borrelia burgdorferi* outer
1072 surface protein C (OspC) binds complement component C4b and confers bloodstream
1073 survival. *Cell Microbiol.* 2017;19. doi:10.1111/cmi.12786
- 1074 75. Xu Q, McShan K, Liang FT. Essential protective role attributed to the surface lipoproteins of
1075 *Borrelia burgdorferi* against innate defences. *Mol Microbiol.* 2008;69: 15–29.
- 1076 76. Tilly K, Bestor A, Rosa PA. Lipoprotein succession in *Borrelia burgdorferi*: similar but
1077 distinct roles for OspC and VlsE at different stages of mammalian infection. *Mol Microbiol.*
1078 2013;89: 216–227.
- 1079 77. El-Hage N, Babb K, Carroll JA, Lindstrom N, Fischer ER, Miller JC, et al. Surface exposure
1080 and protease insensitivity of *Borrelia burgdorferi* Erp (OspEF-related) lipoproteins.
1081 *Microbiology.* 2001;147: 821–830.
- 1082 78. Stevenson B, El-Hage N, Hines MA, Miller JC, Babb K. Differential binding of host
1083 complement inhibitor factor H by *Borrelia burgdorferi* Erp surface proteins: a possible
1084 mechanism underlying the expansive host range of Lyme disease spirochetes. *Infect*
1085 *Immun.* 2002;70: 491–497.
- 1086 79. Lin Y-P, Bhowmick R, Coburn J, Leong JM. Host cell heparan sulfate glycosaminoglycans
1087 are ligands for OspF-related proteins of the Lyme disease spirochete. *Cell Microbiol.*
1088 2015;17: 1464–1476.
- 1089 80. Pereira MJ, Wager B, Garrigues RJ, Gerlach E, Quinn JD, Dowdell AS, et al. Lipoproteome
1090 screening of the Lyme disease agent identifies inhibitors of antibody-mediated complement
1091 killing. *Proc Natl Acad Sci U S A.* 2022;119: e2117770119.
- 1092 81. Grillon A, Scherlinger M, Boyer P-H, De Martino S, Perdriger A, Blasquez A, et al.
1093 Characteristics and clinical outcomes after treatment of a national cohort of PCR-positive
1094 Lyme arthritis. *Semin Arthritis Rheum.* 2018. doi:10.1016/j.semarthrit.2018.09.007
- 1095 82. Livey I, Gibbs CP, Schuster R, Dorner F. Evidence for lateral transfer and recombination in
1096 OspC variation in Lyme disease *Borrelia*. *Mol Microbiol.* 1995;18: 257–269.
- 1097 83. Qiu W-G, Martin CL. Evolutionary genomics of *Borrelia burgdorferi* sensu lato: findings,
1098 hypotheses, and the rise of hybrids. *Infect Genet Evol.* 2014;27: 576–593.
- 1099 84. Balding DJ. A tutorial on statistical methods for population association studies. *Nat Rev*
1100 *Genet.* 2006;7: 781–791.

- 1101 85. Lippert C, Listgarten J, Liu Y, Kadie CM, Davidson RI, Heckerman D. FaST linear mixed
1102 models for genome-wide association studies. *Nat Methods*. 2011;8: 833–835.
- 1103 86. Zhou X, Stephens M. Genome-wide efficient mixed-model analysis for association studies.
1104 *Nat Genet*. 2012;44: 821–824.
- 1105



[Click here to access/download](#)

Supporting Information - Compressed/ZIP File Archive
Supplemental_Data.zip

